Dalton Transactions

Accepted Manuscript

This is an *Accepted Manuscript*, which has been through the Royal Society of Chemistry peer review process and has been accepted for publication.

Accepted Manuscripts are published online shortly after acceptance, before technical editing, formatting and proof reading. Using this free service, authors can make their results available to the community, in citable form, before we publish the edited article. We will replace this *Accepted Manuscript* with the edited and formatted *Advance Article* as soon as it is available.

You can find more information about *Accepted Manuscripts* in the Information for Authors.

Please note that technical editing may introduce minor changes to the text and/or graphics, which may alter content. The journal's standard Terms & Conditions and the Ethical guidelines still apply. In no event shall the Royal Society of Chemistry be held responsible for any errors or omissions in this *Accepted Manuscript* or any consequences arising from the use of any information it contains.

ROYAL SOCIETY OF CHEMISTRY

www.rsc.org/dalton

Dalton Transactions

RSCPublishing

PAPER

Optimized synthesis of *tert.*-butyl-phenyl-substituted Tetrapyridophenazine Ligand and its Ru(II) complexes and determination of dimerization behaviour of the complexes through supramolecular "Fingerhakel" †

Cite this: DOI: 10.1039/x0xx00000x

Received 00th January 2012,
Accepted 00th January 2012

DOI: 10.1039/x0xx00000x

www.rsc.org/

K. Ritter,[a] C. Pehlken,[a] D. Sorsche,[a] and S. Rau*[a]

The synthesis of **tpphz(tbp)$_2$** (tpphz(tbp)$_2$ = 3,16-di(*tert.*-butyl-phenyl)-tetrapyrido[3,2-a:2',3'c:3'',2'',- h:2''',3'''-j]phenazine) has been optimized by using a new synthetic route. The complexes **Ru(tbp)$_2$tpphz**, **Rutpphz(tbp)$_2$**, **Rutpphz(tbp)$_2$Ru** and the reference compound **Ru(tbp)$_2$phen** (where Ru = (tbbpy)$_2$Ru, tbbpy = 4,4'-di-*tert.*-butyl-2,2'-bipyridine and (tbp)$_2$phen = 3,8-Bis(4-*tert.*-butyl-phenyl)-1,10-phenanthrolin) have been synthesized and characterized. Crystal structures or structural motives could be received for each intermediate and complex and for the first time a tpphz based uncomplexed ligand could be investigated in the solid state. The mononuclear complexes **Ru(tbp)$_2$tpphz** and **Rutpphz(tbp)$_2$** form π-π stacked dimers in the solid state. The latter exhibits an interesting aggregation in the solid state with three π-interactions. Concentration dependent aggregation of these isomers in solution is observed with the aid of ^{1}H-NMR investigations. Out of those dimerization constants (K_D) could be calculated for the complexes **Ru(tbp)$_2$tpphz** and **Rutpphz(tbp)$_2$**. The values differ significant. Photophysical and electrochemical properties of the presented complexes were investigated and compared with reference compounds. The *tert.*-butyl-phenyl-substitution induces a stabilization of the ^{1}MLCT and ^{3}MLCT states localized on the phenanthroline part of the bridging ligand. The ^{3}MLCT localized on the phenazine portion seems to be not or only to a minor extend influenced by these substituents.

[a] [a] Department of Inorganic Chemistry I, University of Ulm, Albert-Einstein-Allee 11, 89081 Ulm, Germany. Email: sven.rau@uni-ulm.de.

† Fingerhakeln is an old athletic sport practiced in the region of german-speaking Alps. Fingerhakeln means two people hook one of their fingers with each other and each tries to pull the other to his side.

Electronic Supplementary Information (ESI) available: concentration dependent ^{1}H-NMR spectra, peak assignment in the ^{1}H-NMR spectra, details on the calculation of the dimerization constant K_D and on the single crystal structure refinement. For ESI and crystallographic data in CIF or other electronic format see DOI: 10.1039/c000000x/

Dalton Transactions Accepted Manuscript

Introduction

To avoid strong climatic changes induced by consumption of fossil fuels carbon-neutral energy production has to be developed. A rich energy source is the solar energy which is by far the largest exploitable resource.[1,2] Solar cells or solar thermal collectors are already used worldwide but they only work on sunny days and a second energy source is needed for the nights or rainy and cloudy days.

A storage device for solar energy would enable the use of solar energy based resources independent of weather and daytime. An attractive and clean solution is the development of a sunlight-driven water splitting catalyst to get access to oxygen and hydrogen whereas the latter can serve as fuel.[1,3,4]

The production of hydrogen with a catalyst based on a photochemical molecular device is a rapidly developing research area.[1,3,5] Here light is absorbed by a photoactive center and charge-separation is taking place, followed by electron transfer towards a catalytic center where the electrons are used to produce hydrogen out of protons. The photocatalytic center needs to be recycled by an electron donor.

Different photochemical molecular devices were already investigated which catalyze hydrogen production under irradiation and in presence of sacrificial electron donor.[6-11] A well investigated example is RutpphzPd (where Ru = $(tbbpy)_2Ru$, tbbpy = 4,4'-di-*tert*.-butyl-2,2'-bipyridine, tpphz = tetrapyrido[3,2-a:2',3'c:3'',2'',-h:2''',3'''-j]phenazine, Pd = $PdCl_2$).[12-16] The catalyst works with the maximum turnover number of 238[16] based on the optimized interplay of all components. Ruthenium polypyridine complexes exhibit high chemical stability and photo-redox activity and are used as photosensitizer.[17,18] The catalytic center Pd was chosen as it is known to be capable of producing hydrogen under reducing conditions.[19]

The third component, the bridging ligand plays an important role in supramolecular devices as it has to achieve a desired vectorial electron or energy transfer.[11] Tpphz, see Figure 1, supports an electron transfer in RutpphzPd on a subnanosecond timescale[12] which proceeds in the following manner: The phenanthroline part which is bound to Ruthenium is involved in the ^{1}MLCT (metal to ligand charge transfer) and in the following ^{3}MLCT relaxation. This is followed by an intra ligand charge transfer to the phenazine part of tpphz and from there the electron can move to the catalytic subunit.[20-22] It is known that the phenazine part of tpphz is electronically decoupled from the phenanthroline parts.[6,23]

A correlation between initial localization of the excited state (either on the peripheral *tert*.-butyl-bipyridine ligands or on the phenanthroline part of the bridging ligand tpphz) and the amount of hydrogen formed is observed. The initial localization of the excited state depends on the excitation wavelength.[13] Based on these detailed investigation it has been suggested that a high portion of a bridging ligand localized excited state would generate a more active photo catalyst.

To increase the amount of the bridging-ligand localized excited state bromine substituents were introduced in 3,16-position of the tpphz ligand. This asymmetric scaffold presents two different binding sites of tpphz resulted in two isomeric complexes, $RutpphzBr_2$ and $RuBr_2tpphz$ (where Ru = $(tbbpy)_2Ru$, tbbpy = 4,4'-di-*tert*.-butyl-2,2'-bipyridine and Br_2tpphz = 3,16-di-bromo-tetrapyrido[3,2-a:2',3'c:3'',2'',- h:2''',3'''-j]-phenazine).[24] The therefrom arisen photo catalyst $RuBr_2tpphzPd$ (where Pd =$PdCl_2$) showed stabilized states (^{1}MLCT and ^{3}MLCT) located on the substituted phenanthroline portion of tpphz which is bound to Ruthenium. However less catalytic activity potentially caused by a slower electron transfer across the bridge were observed. Obviously the bromine-substituents trapped the electron at the substituted phenanthroline portion.[16]

Another idea was to enlarge the aromatic system at the Ruthenium binding site of the bridging ligand and **tpphz(tbp)$_2$** was synthesized (where tpphz(tbp)$_2$ = 3,16-di(*tert*.-butyl-phenyl)-tetrapyrido[3,2-a:2',3'c:3'',2'',- h:2''',3'''-j]phenazine, see scheme 1).[24] Yet the yield of the reaction was quiet low (12 %) and the purification of the Ruthenium complexes was not achieved.[24]

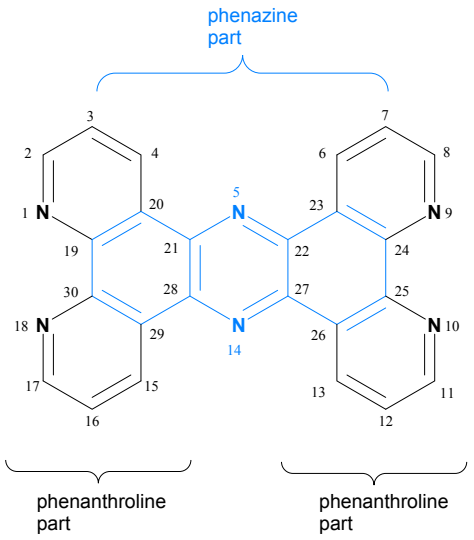

Figure 1: Labeled tpphz.

The 4-methoxyphenyl substitution in position 2,17 of tpphz was also performed and resulted in the photo catalyst Ru(bmptpphz)Pd (where Ru = $(tbbpy)_2Ru$, tbbpy = 4,4'-di-*tert*.-butyl-2,2'-bipyridine, bmptpphz = 2,17-bis(4-methoxy-phenyl)tetrapyrido[3,2-a:2',3'-c:3'',2''-h:2''',3'''-j]phenazine and Pd = $PdCl_2$).[25,26] In this catalyst Palladium is bound to the substituted phenanthroline part of tpphz in a tridentate NNC-coordination motif. This leads to an increased stability of the Palladium binding to the ligand but the catalytic activity with the maximum turn over number of 50 is decreased compared to RutpphzPd.[26]

A further variation on the tpphz is the "exchange" of one nitrogen-atom localized on the phenazine part against a carbon atom to investigate the role of the nitrogen in this position. Rutpac (where Ru = $(tbbpy)_2Ru$, tbbpy = 4,4'-di-*tert*.-butyl-2,2'-bipyridine, tpac = tetrapyrido[3,2-a:2',3'-c:3'',2''-h:2''',3'''-j]acridine) and RutpacPd (where Pd = $PdCl_2$) was synthesized and characterized. The results showed less catalytic activity but a comparable fast electron transfer across the bridging ligand.[14]

The introduction of methyl-groups in 4,15-position of tpphz was achieved and does not influence the absorption and emission properties.[27]

Another motivation to synthesise derivatives of tpphz is the possibility of tpphz complexes to form π-stacks[23] which is also observed for other metal complexes with large aromatic ligands.[28-31] Indeed tpphz like molecules probably exhibit the π-stacking aggregation also without the metal, but due to the bad solubility of tpphz this could not been evidenced until now.

The property of π-aggregation[32] is useful for the formation of a supramolecular architecture in solution or in the solid phase, in organic or complex chemistry and also in the nature.[33,34] Examples for already investigated applications where this feature is crucial are crystal engineering[35,36], organic electronics[37,38] and intercalation of metal-complexes into DNA.[39]

Tpphz is a heteroacene and interesting for electron transport within organic semiconductors[37,40]. Thereby the overlap of the π-face may be important for the magnitude of the transfer integral.[37,41] The substitution on large aromatic molecules is known to provide control over molecular organization.[38] The lack of a molecular crystal structure of tpphz made it impossible to evaluate this molecule with regard to electron transport.

The binding of a Ruthenium polypyridyl complex to a large aromatic ligand leads also to interesting implementations using the property of π-interaction like DNA intercalation and cleavage under irradiation or metallo-supramolecular aggregation.[36,42-46]

Dalton Transactions Accepted Manuscript

This journal is © The Royal Society of Chemistry 2012

One example is a water oxidation catalyst whose suggested mechanism includes the dimerization of two Ruthenium-complexes in solution.[47] It is further shown that π-π-interactions between coordinated axially isoquinolines are of mechanistic significance as they stabilize the dimer.[48]
We present the improved synthesis and characterization of **tpphz(tbp)$_2$** and its Ruthenium(II) complexes and of the reference compound **Ru(tbp)$_2$phen**.

Results and Discussion

Ligand-synthesis

Tpphz(tbp)$_2$ is a literature known compound[24] where the synthesis was achieved via a Suzuki cross-coupling reaction of Br_2tpphz with 4-*tert*.-butyl-phenyl-boronic acid. However, low yields (12 %) were obtained probably due to insufficient solubility of Br_2tpphz.
To improve the yields and to avoid the low solubility of Br_2tpphz we tried to introduce the phenyl-substituents earlier in the synthesis.
First we used 3,8-dibromo-1,10-phenanthroline as starting compound which is literature known[24], performed the Suzuki cross-coupling reaction with 4-*tert*.-butyl-phenyl-boronic acid[49] and obtained 3,8-bis(4-*tert*.-butyl-phenyl)-1,10-phenanthrolin (**phen(tbp)$_2$**). The oxidation of this product to phen(tbp)$_2O_2$ (see Scheme 1) as described by Ott failed in our hands.[50]
Our next attempt was to introduce the dione-functionalization before the phenyl residues. This procedure worked and is depicted in Scheme 1. All compounds were characterized with the aid of NMR and the purity was checked with elemental analysis. Crystal structures or motives of each compound demonstrated the right interpretation of the NMR-measurements.
We started with the literature known compound phenBr_2O_2.[24] This molecule is described to be instable[24] so we protected the dione group with a literature known method[25] to obtain the more stable phenBr_2O_2X.
In the next step phenBr_2O_2X was converted with 4-*tert*.-butyl-phenyl-boronic acid in a Suzuki cross-coupling reaction to phen(tbp)$_2O_2$X. However, the outcome of the reaction depends strongly on the production batch of the palladium precursor, $Pd_2(dba)_3$, and there might be high deviation in the yield.
The de-protection of phen(tbp)$_2O_2$X was achieved as known from literature[25]. Two species are observed as the products: the desired phen(tbp)$_2O_2$ and 3,8-Bis(4-*tert*.-butyl-phenyl)-1,10-phenanthrolin-5,6-diole (phen(tbp)$_2OH_2$) as a by-product in yields 51 % and 45 % respectively.
The last step of the ligand synthesis is the literature known condensation of phen(tbp)$_2O_2$ with 1,10-phenanthroline-5,6-diamine which proceeds with yields of 93 %.[24]
As previously described, tpphz(tbp)$_2$ shows improved solubility compared to tpphz.[24] ^{1}H-NMR data matches well with the literature known spectrum except a slight shift of the signals probably caused by the concentration dependency of the chemical shift.[24]

Complexes-synthesis

The synthesis of **Ru(tbp)$_2$tpphz** and **Rutpphz(tbp)$_2$** was performed as the synthesis of other Rutpphz analogues[24,49]. However ethanol could be used instead of ethylenglycol due to the better solubility of **tpphz(tbp)$_2$** compared to the unsubstituted tpphz.
Both complexes, **Ru(tbp)$_2$tpphz** and **Rutpphz(tbp)$_2$**, were detected in the crude product with the aid of ^{1}H-NMR in a ratio of 70/30 respectively. Obviously the phenyl-substituted phenanthroline part of the ligand is preferred for coordination. The reason might be the +I-effect of the *tert*.-butyl-pheny-groups which leads to enhanced electron-density on the phenanthroline portion and maybe to a stronger attraction of the Ru(tbbpy)$_2^{2+}$ mojety.

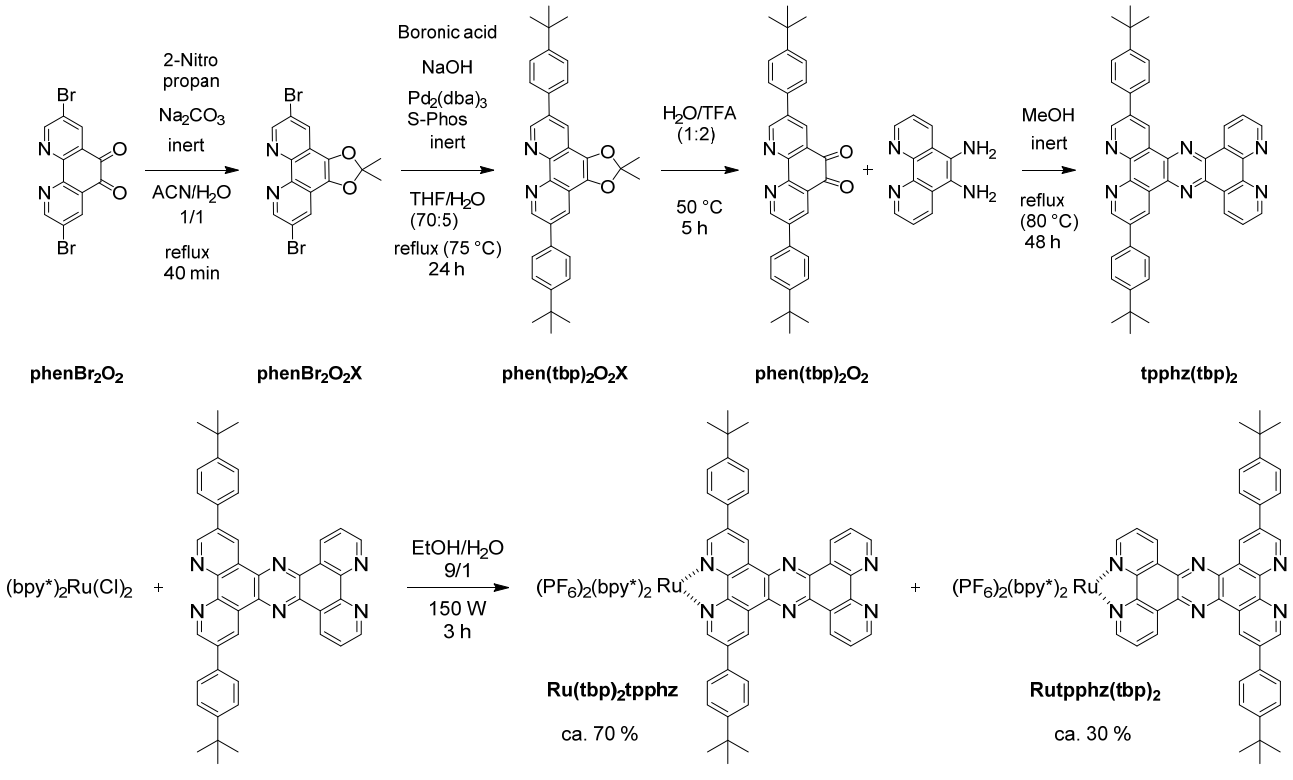

Scheme 1: Synthetic route towards the complexes Ru(tbp)$_2$tphhz and Rutpphz(tbp)$_2$.

Dalton Transactions Accepted Manuscript

The reaction proceeds with full conversion and only small impurities could be obtained beside the two isomers in the NMR spectrum of the crude product. However, it is very difficult to separate the isomers from each other, what is already described in literature[24] probably because of the π-stacking that is known for tpphz-complexes.[23] The usual separation methods (column chromatography, silica, acetonitrile (ACN)/H_2O with potassium-nitrate) did not work reproducible. F. Keene used aromatic anions to separate even diastereomers of Ruthenium-complexes on a cation exchange chromatography.[51] We tried to utilize this method on silica in hoping to disturb the π-stacks by the aromatic counter ions. We found benzosulfonate as counter ion and sodiumbenzosulfonate present in the mobile phase to work, but the two isomers separate very late on the column and diffuse in broad bands so just small amounts can be purified in one attempt.
To gain **Ru(tbp)$_2$tpphzRu** a literature known procedure was performed.[23] The synthesis was straight forward as well as the synthesis of **Ru(tbp)$_2$phen**.[24]

Crystal structures and motives

From all new synthesized molecules crystals could be grown and the structures could be resolved with good R-values except for **tpphz(tbp)$_2$** and **Ru(tbp)$_2$tpphzRu** where only a structural motif could be generated. All synthesized molecules except **Ru(tbp)$_2$phen** and **Ru(tbp)$_2$tpphzRu** show π-aggregation in their crystal structures. The structures are depicted in Figure 2. Table 1 shows detailed listing of some bond lengths and angles for comparison. Figure 1 shows the atom-labeling, which is used in Table 1

Ligands

The respective distances and the angels shown in Table 1 do not deviate significantly between the different structures. This reveals that neither different substitution in 3,8-position of the phenanthroline (portion) nor the protection of the dione nor the coordination of a Ruthenium center influence the bond-lengths and -angles in the phenanthroline- or the tpphz-core significantly. Only the C4-C20-C26-C13-angle deviates noticeable from 180 ° and thus from a complete planar tpphz in the structures of **Ru(tbp)$_2$tpphz** and **Rutpphz(tbp)$_2$** (details see below).
Tpphz(tbp)$_2$ aggregates in endless leaning piles which are connected with each other via short contacts with dichloromethane. Figure 3 shows the solid state aggregation of **tpphz(tbp)$_2$**.
The stacked **tpphz(tbp)$_2$** exhibits an overlap over almost the entire molecule in spite of the bulky substituents as these are changing the location by a 180 ° flip of the molecule. Thus soluble tpphz derivatives may be applicable in the field of organic electronics (see introduction).

Complexes

The geometry around the Ru-center in the structures does not deviate significantly from other similar complexes.[52]
Both **Ru(tbp)$_2$tpphz** and **Rutpphz(tbp)$_2$** exhibit in the solid state a dimer-structure where two molecules stack together attracted by π-π-interaction. The dimer structures are shown in figure 3.
The dimer observed in the solid state structure of **Ru(tbp)$_2$tpphz** exhibits a π-π-interaction along the tpphz plane similar to the pattern observed for **Rutpphz**.[6]
However, the dimer of **Rutpphz(tbp)$_2$** possesses two additional π-interactions: the phenyl-rings on the two sides of the stacked tpphz-plane do interact with each other. There is a C-H···π contact in each phenyl-phenyl-interaction (see Figure 3C). The angle between the phenyl-rings is 58.1°. The centroids-distance of the phenyl-rings is with 5.549 Å within the typical values for this type of interaction.[34,53] These three π-interactions, two CH-π and one π-π, indicate a different aggregation compared to one π-π-interaction.
The phenyl rings rotate out of the respectively planes with the torsion angles in the range of 27°-42°. This is due to a compromise between stabilization by conjugation and the lowest repulsion between the Hydrogen-atoms of the pyridine and phenyl rings as suggested in literature.[24] Interesting is however that one phenyl-ring in the structure of phen(tbp)$_2O_2$ exhibits a torsion angle of only 9.4°. This indicates a relatively free rotation of the *tert*.-butyl-phenyl-substituent in solution. The sharp signal-shape of the ^{1}H-NMR signals of in the phenyl rings denotes the same.

Dimerization constant

Similar to **Rutpphz**, these substituted complexes also show a concentration dependency in ^{1}H-NMR experiments. Therefore a series of ^{1}H-NMR spectra of the two complexes in deuterated acetonitrile in a concentration range from $3*10^{-2}$ to $3*10^{-5}$ mol/l were recorded. Concentration dependent ^{1}H-NMR spectra of **Rutpphz(tbp)$_2$** are shown in Figure 4 (Spectra of **Ru(tbp)$_2$tpphz** and assignment of the peaks are shown in the supporting information). The concentration dependent shift of the signals of the aromatic protons appears due to aggregation of the complexes.
These shifts are used for the calculation of the equilibrium constant of the dimerization of the complexes (K_D). For this purpose non linear least squares global curve fitting was applied to the dataset, similar to the work of Dixon et al. and Chen et al. (for details, see supporting information).[54,55]
Table 2 shows the determined dimerization constants (K_D) of **Rutpphz(tbp)$_2$**, **Ru(tbp)$_2$tpphz** and the reference compound **Rutpphz**.[57]

Table 1: Selected details of the crystal structures, distances are given in pm, angels and dihedral angles in degrees.

	N1[a]-C2	C8-N9	C19-C30	C24-C25	N1-C19-C20	C21-C20-N5	C4-C20-C26-C13
phenBr$_2$O$_2$X	1.319(5)	/	1.440(6)	/	121.6(4)	/	/
phen(tbp)$_2$O$_2$X	1.318(2)	/	1.447(2)	/	121.1(2)	/	/
phen(tbp)$_2$O$_2$	1.332(2)	/	1.479(2)	/	121.7(1)	/	/
phen(tbp)$_2$	1.314(3)	/	1.440(3)	/	121.6(2)	/	/
Ru(tbp)$_2$phen	1.325(3)	/	1.423(3)	/	122.6(2)	/	/
Ru(tbp)$_2$tpphz	1.343(4)	1.321(4)	1.447(4)	1.474(4)	122.9(2)	117.0(2)	173.3(3)
Rutpphz(tbp)$_2$	1.345(5)	1.312(5)	1.447(5)	1.457(5)	123.3(3)	116.6(3)	171.4(4)

[a] N1 is the nitrogen that is bound to Ruthenium in the case of the mononuclear complexes.

Dalton Transactions Accepted Manuscript

This journal is © The Royal Society of Chemistry 2012

Dalton Transactions RSCPublishing

PAPER

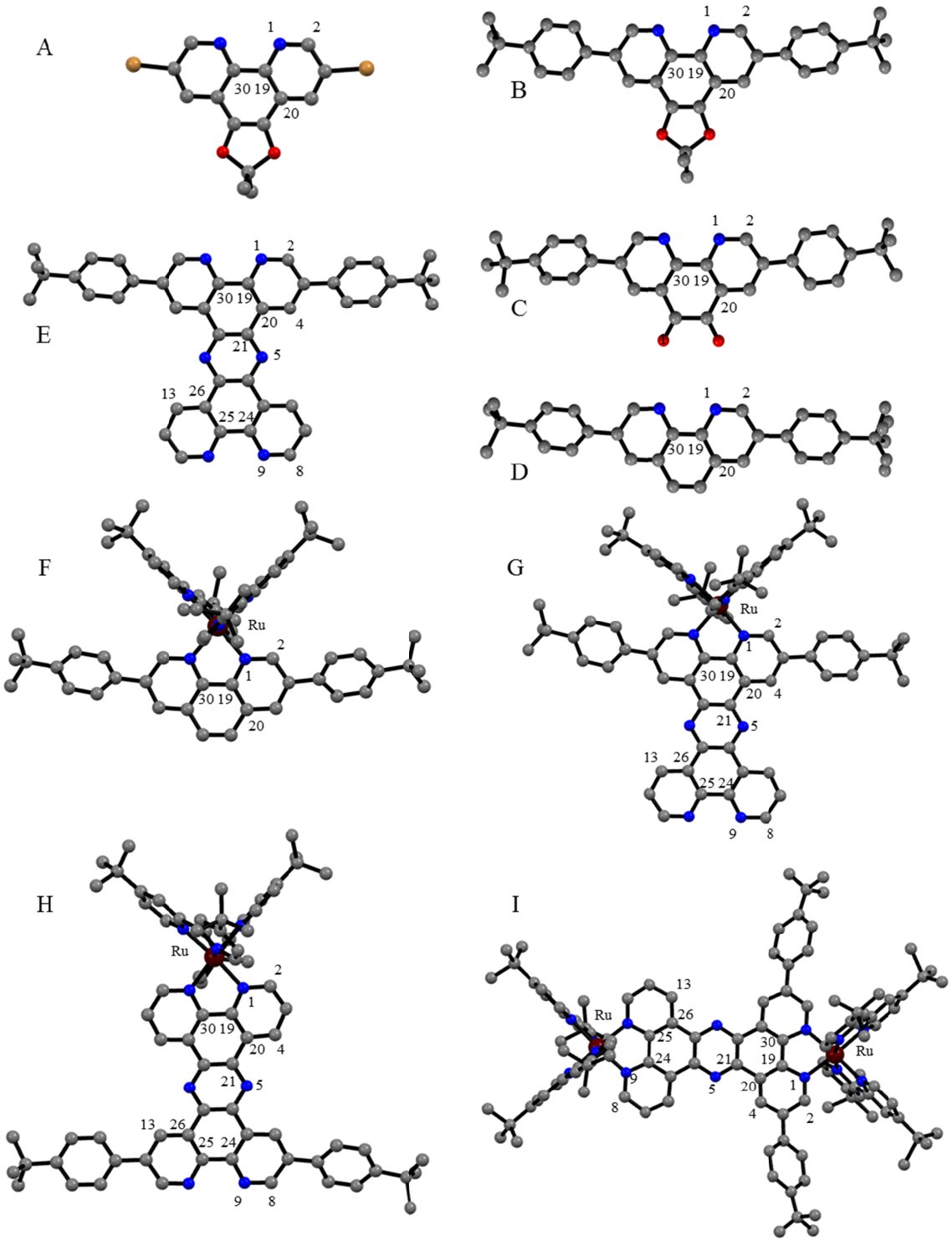

Figure 2: Molecular structures or motives of A: phenBr_2O_2X, B: phen$(tbp)_2O_2X$, C: phen$(tbp)_2O_2$, D: phen$(tbp)_2$, E: **tpphz$(tbp)_2$**, F: **Ru$(tbp)_2$phen**, G: **Ru$(tbp)_2$tpphz**, H: **Rutphhz$(tbp)_2$**, I: **Ru$(tbp)_2$tpphzRu**. PF_6-anions and solvent-molecules are omitted for clarity; Nitrogen is blue-colored, Ruthenium dark-red, Oxygen red and Bromine brown.

Dalton Transactions Accepted Manuscript

Dalton Transactions RSCPublishing

PAPER

Table 2: dimerization constants of **Rutpphz**, **Rutpphz(tbp)$_2$** and **Ru(tbp)$_2$tpphz**.

	Rutpphz	**Ru(tbp)$_2$tpphz**	**Rutpphz(tbp)$_2$**
K_D [M^{-1}]	289 ± 17[56,57]	647 ± 46	3634 ± 176

The dimerization constant of **Ru(tbp)$_2$tpphz** is doubled compared to **Rutpphz**, which is likely due to the enlargement of the aromatic system. Surprisingly, **Rutpphz(tbp)$_2$** exhibits a tenfold higher dimerization constant compared to **Rutpphz**. As an identical aromatic system is present in both complexes an additional effect has to be taken into consideration.

The molecular structure in the solid state showed a different aggregation mode between **Rutpphz(tbp)$_2$** and **Ru(tbp)$_2$tpphz**. We suggest that the exhibition of two additional π-interactions in the case of **Rutpphz(tbp)$_2$** occurs not only in the solid state but also in the solution and stabilizes the dimerized form strongly which is obvious in the dimerization constant.

This effect can be compared with the chelate effect or the hydrogen-bonding: the more individual interactions or bondings occur between two molecules the stronger association exists between them.

The molecular crystal structure of **tpphz(tbp)$_2$** does not exhibit the CH-π-stacking of the phenyl rings which is observed in the molecular crystal structure of the complex **Rutpphz(tbp)$_2$**. The reason might be that in the complex only a part of the overlapping area of the tpphz-planes can be used for π-interaction due to the large Ru(tbbpy)$_2$ portions. And obviously it is advantageous for the complex to lose a little bit more of the overlapping area and to gain two additional π-interactions. But in the solid state of the ligand **tpphz(tbp)$_2$** it seems to be more stable for the system to utilize almost the whole tpphz plane instead of diminish the overlapping area for the sake of additional π-interactions of the phenyl-groups.

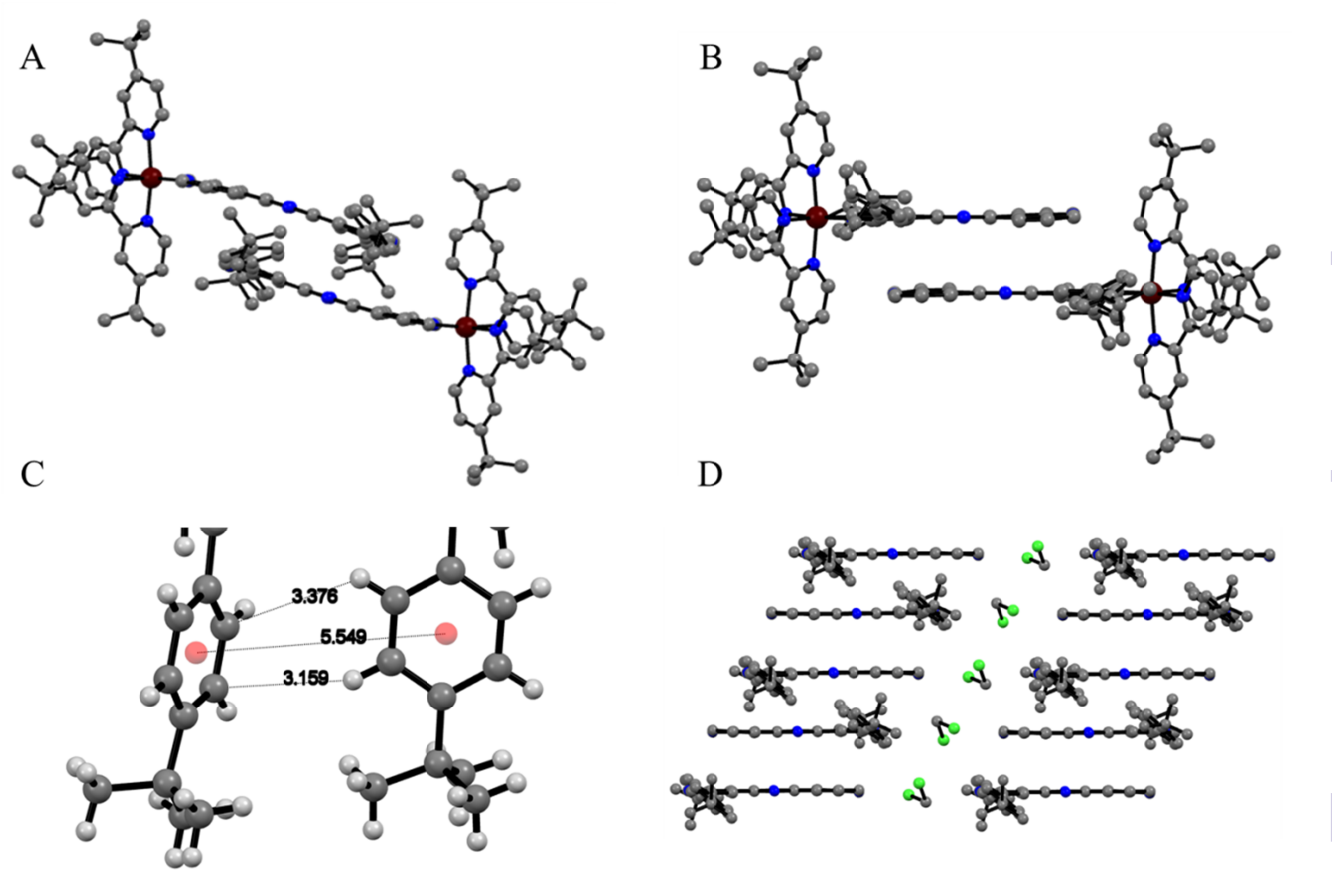

Figure 3: A) Molecular structure of a cation dimer Rutpphz(tbp)$_2$ in the solid state; B) Molecular structure of a cation dimer of Ru(tbp)$_2$tpphz in the solid state; C) Detailed view on the C-H···π contact between the phenyl-rings of two dimerized Rutpphz(tbp)$_2$ D) Molecular packing of the ligand tpphz(tbp)$_2$ in the solid state with dichloromethane between the leaning piles; Nitrogen is blue-colored, Ruthenium dark-red and Chloride green.

Dalton Transactions Accepted Manuscript

Dalton Transactions RSCPublishing

PAPER

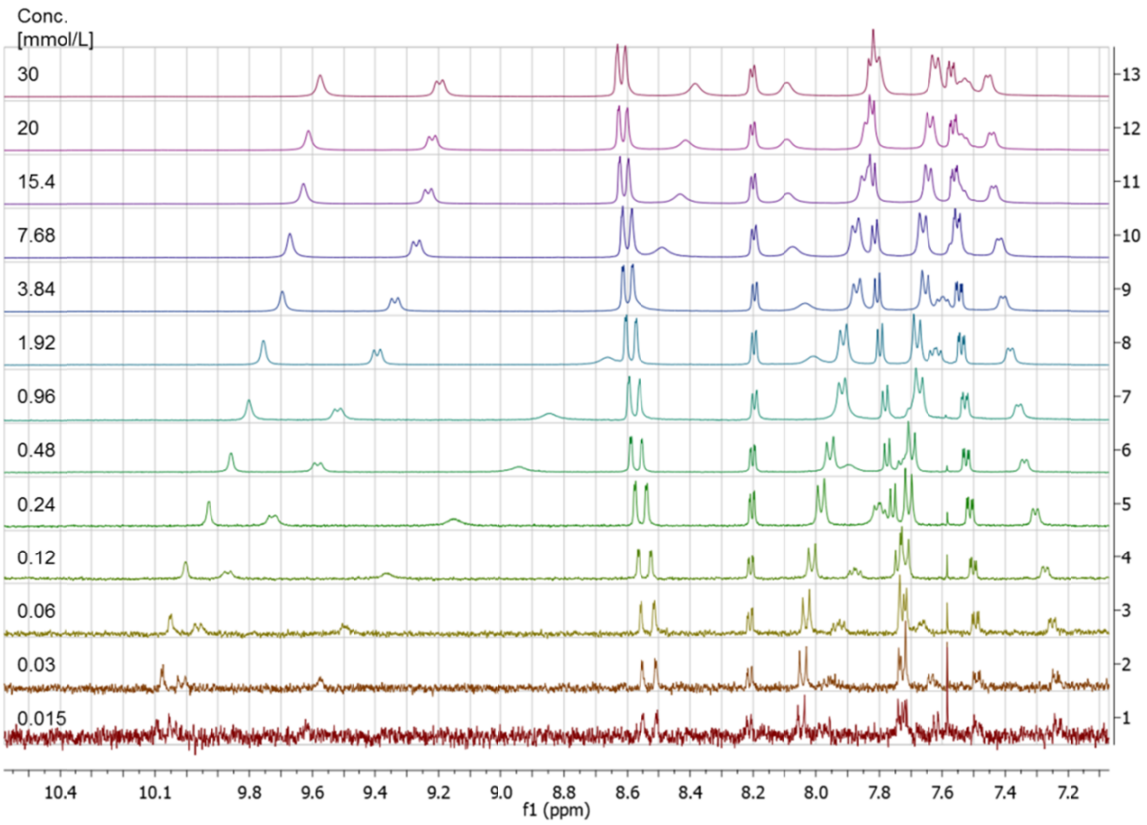

Figure 4: Concentration dependent ^{1}H-NMR spectra of **Rutpphz(tbp)$_2$** as a PF_6 salt in Acitonitrile.

UV/vis absorption spectroscopy of the ligands

The absorption and emission data of the synthesized molecules and reference compounds in dichloromethane (DCM) and mostly ACN are listed in Table 3. The spectra of phen(tbp)$_2$ and **tpphz(tbp)$_2$** are shown in the supporting information. The ligands are not soluble in ACN.

Phen(tbp)$_2$ shows a phenanthroline (phen) centered π→π* transition at 275 nm that appear in the absorption spectrum of phen (265 nm) as well.[59] The second absorption maximum at 328 nm is caused by the phenyl-substitution as in the phen spectrum this band is absent but in the spectrum of 3,8-Bis[{3,5-bis(triflouromethyl)}phenyl]-1,10-phenanthroline (phen((tFm)$_2$ph)$_2$) similar band is present (321 nm).[59] The small difference of 7 nm might be caused by electron donating- and electron with-drawing substitution of the phenyl-rings. A band at similar wavelength appears in the spectrum of phen(tbp)$_4$ as well (335 nm).[49]

The absorption bands observed in the spectrum of phen(tbp)$_2$ (275 nm and 328 nm) appear in the spectrum of **tpphz(tbp)$_2$** as well (273 nm and 330 nm) accompanied by further absorption maxima (302 nm; 368 nm; 377 nm; 390 nm) which can be assigned to the phenazine part of **tpphz(tbp)$_2$** and can also be found in the spectrum of tpphz.[24]

The literature known spectrum of **tpphz(tbp)$_2$** deviates from our data.[24] A possible reason for that might be an aggregation of the molecules caused by the π-attraction. We performed more detailed experiments with **tpphz(tbp)$_2$** where a solution of **tpphz(tbp)$_2$** was kept for several days under ambient conditions and analysed it with the absorption and emission spectroscopy. A change in the spectra was monitored (more details are presented in the supporting information). The literature known absorption spectrum[24] equals the absorption of the **tpphz(tbp)$_2$** which was dissolved for several days.

UV/vis absorption spectroscopy of the complexes

The spectra of the complexes are shown in figure 5 and the band maxima are listed in table 3. Only the spectra measured in DCM are discussed as they are similar to those in ACN.

All the complexes presented here exhibit a band around 285 nm which is due to tbbpy- and phenanthroline-centered π→π* transition.[24]

The absorption maximum at around 320 nm of **Ru(tbp)$_2$tpphz** and **Rutpphz(tbp)$_2$** which is only slightly influenced by the location of the substitution (difference 9 nm) and absent in **Ru(tbp)$_2$phen** is a tpphz centered transition and also observed for similar systems.[24,58]

The band around 350 nm that appear in all **tpphz(tbp)$_2$**-complexes and in **Ru(tbp)$_2$phen** is caused by the phenyl substituents. In the absorption spectrum of Rutpphz, $RuBr_2$tpphz and RutpphzBr_2 this band is absent.[24] Similar bands are observed in the spectra of

Dalton Transactions Accepted Manuscript

phen(tbp)$_2$ and **tpphz(tbp)$_2$** with comparable intensities but blue shifted. The extent of the shift of the band upon coordination is comparable for **Ru(tbp)$_2$phen** and **Ru(tbp)$_2$tpphz** (26 nm and 32 nm respectively) and less pronounced for **Rutpphz(tbp)$_2$** (10 nm). The shift of the band is caused by the Ruthenium moiety and the extent of the shift correlates with the distance of the substitution and the Ruthenium moiety.

In the case of phen(tbp)$_4$ also a red shift of the analogous band upon coordination is observed though less pronounced (17 nm)[49]. Interesting is that the analogous absorption-band at 322 nm of the electron with-drawing phen((tFm)$_2$ph)$_2$ is not influenced by the coordination to Ruthenium-center[59] what may be due to the electron-withdrawing effect of the two CF_3 groups on each phenyl substitutent.

The absorption between 400 nm and 600 nm in a Ruthenium-polypyridyl complex is due to metal-to-ligand-charge-transfer (^{1}MLCT).[24]

In the case of Ruphen and its derivatives the ^{1}MLCT is not influenced by electron-donating substituents (*tert*.-butyl-phenyl) whereas electron withdrawing substitution (3,5-bis(triflouromethyl)phenyl) leads to red shift of 30 nm compared to unsubstituted Ruphen. This shows a clear stabilization of the phenanthroline localized ^{1}MLCT in the latter complex.[59]

The ^{1}MLCT of Rutpphz, **Rutpphz(tbp)$_2$**, **Ru(tbp)$_2$tpphz** and **Ru(tbp)$_2$tpphzRu** deviates only by the appearance of a shoulder around 480 nm in the spectrum of **Ru(tbp)$_2$tpphz** which also appears in the in the case of RuBr$_2$tpphz[24]. This indicates a stabilization of ^{1}MLCT localized on the bridging ligand. The absence of this shoulder in the spectrum of **Rutpphz(tbp)$_2$** and RutpphzBr$_2$ due to the spatial distance of the substitution indicates very limited electronic communication across the tpphz.[24]

It is however peculiar that this shoulder at 480 nm which appears in **Ru(tbp)$_2$tpphz** due to the substitution on the phenanthroline part of tpphz is absent in **Ru(tbp)$_2$phen**.

Table 3: Absorption and emission maxima of synthesized molecules and reference compounds.

Compound	solvent	Absorption λ_{max}/nm (Extinction Coefficient ($\varepsilon/10^3 M^{-1}cm^{-1}$))	Emission[a] λ_{max}/nm
phen[b]	DCM	265 (32)	365
phen(tbp)$_2$	DCM	275 (48); 328 (36)	387
phen((tFm)$_2$ph)$_2$[b]	DCM	278 (37); 321 (23)	391
phen(tbp)$_4$[c]	DCM	265 (37); 300 (47); sh[d] 335 (29)	408
tpphz[e,f]	DCM	279 (66); 320 (29); 361 (14); 381 (21)	393
tpphz(tbp)$_2$[g]	DCM	273 (70); 302 (54); 330 (57); 368 (19); 377 (19); 390 (23)	473
tpphz(tbp)$_2$[e,g]	DCM	277 (25); 339 (18); 372 (11); 393 (11)	485
tpphzBr$_2$[e,f]	DCM	282 (64); 324 (40); 363 (20); 385 (19)	399
Ruphen	DCM[b]	267 (64); 288 (69); sh[d] 426 (16); 455 (19)	602
	ACN[c]	265 (53); 287 (63); sh[d] 431 (15); 454 (16)	610
Ru(tbp)$_2$phen	DCM	287 (96); 354 (47); sh[d] 437 (16); 456 (17)	612
	ACN	285 (99); 348 (47); 442 (17)	623
Ru((tFm)$_2$ph)$_2$phen[b]	DCM	286 (98); 322 (31); 441 (12); sh[d] 485 (11)	652
Ruphen(tbp)$_4$[c]	DCM	289 (74); sh[d] 310 (38); 325 (34); sh[d] 428 (13); 462 (15)	613
	ACN	288 (80); sh[d] 313 (46); 351 (36); 444 (15)	628
Rutpphz[h,i]	DCM	285 (130); sh[d] 315 (46); 382 (26); 444 (19)	620
	ACN	283 (105); sh[d] 314 (45); 379 (31); 442 (20)	633
Rutpphz[e,h]	DCM	282 (130); sh[d] 315 (46); 377 (26); 444 (19)	629
	ACN	285 (105); sh[d] 318 (45); 381 (31); 445 (20)	638
Ru(tbp)$_2$tpphz	DCM	286 (100); sh[d] 314 (61); 362 (57); 385 (44); 446 (18); sh[d] 483 (13)	628
	ACN	285 (101); sh[d] 312 (59); 351 (58); 384 (40); 443 (17); sh[d] 483 (13)	643
Rutpphz(tbp)$_2$	DCM	284 (119); sh[d] 323 (64); 340 (69); 387 (27); 442 (21)	620
	ACN	283 (119); sh[d] 323 (70); 335 (72); 385 (28); 442 (21)	634
RuBr$_2$tpphz[e]	DCM	285 (98); 318 (46); 389 (19); 438 (16); 480 (12)	650
	ACN	285 (94); 317 (48); 386 (23); 437 (13); 478 (9)	661
RutpphzBr$_2$[e]	DCM	286 (97); 315 (40); 384 (20); 447 (18)	633
	ACN	284 (95); 315 (42); 383 (22); 444 (17)	645
RuBr$_2$tpphzRu[j]	DCM	284; 352; 372; 444	626
	ACN	284; 354; 374; 444	637
RutpphzRu[j]	DCM	285; 352; 371; 449	605
	ACN	283; 351; 371; 445	616
Ru(tbp)$_2$tpphzRu	DCM	284 (175); 345 (74); 448 (42)	648
	ACN	283 (166); 345 (74); 444 (38)	677

[a] λ_{exc}/ligands = 264 nm, λ_{exc}/complexes = 445 nm; [b] from reference [59]; [c] from reference [49]; [d] sh = shoulder; [e] from reference [24]; [f] 0.08 mol/L triflouracetic acid; [g] deviation in the absorption and emission behavior of the equal compound explainable by changing of the absorption and emission properties of the ligand after standing in solution; for further details see supporting information; [h] deviation of the emission of 9 nm occurs due to different measurement device; [i] extinction coefficients from reference[24]; j from reference[62].

Dalton Transactions Accepted Manuscript

This journal is © The Royal Society of Chemistry 2012

Dalton Transactions RSCPublishing

PAPER

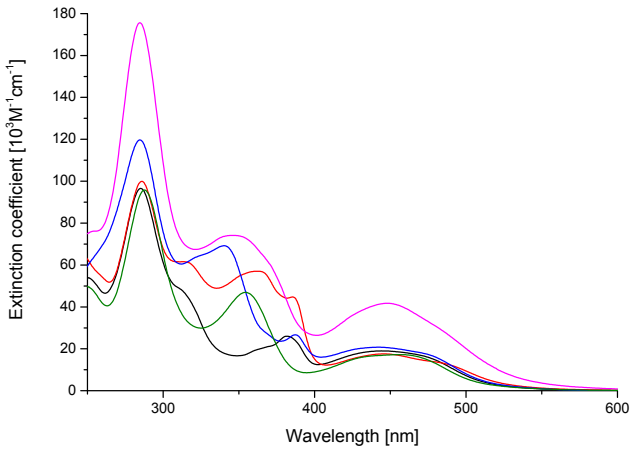

Figure 5: Absorption spectra of Rutpphz (black), **Ru(tbp)$_2$tpphz** (red), **Rutpphz(tbp)$_2$** (blue), **Ru(tbp)$_2$tpphzRu** (pink), Ru(tbp)$_2$phen (green) in DCM.

The absorption of the dinuclear **Ru(tbp)$_2$tpphzRu** is an addition of the spectra of **Ru(tbp)$_2$tpphz** and **Rutpphz(tbp)$_2$**.

Emission spectroscopy

The emission of **phen(tbp)$_2$** at 387 nm is similar to ((tFm)$_2$ph)$_2$phen (391 nm) but different to phen (365 nm)[59] which makes the stabilization of the emissive state through the phenyl substitution obvious. The emission of the fourfold substituted phen(tbp)$_4$ is rather different (408 nm).[49]

The emission of **tpphz(tbp)$_2$** at 473 nm is quite different to tpphz and tpphzBr$_2$ (393 nm and 399 nm respectively).[24] The literature known spectrum of **tpphz(tbp)$_2$** deviates from our data.[24] A possible reason for that is described above and shown in the supporting information.

The emission of Ruthenium-polypyridyl complexes is assigned to decay from a ^{3}MLCT excited state that is localized on one of the ligands.[60] The emission of **Ru(tbp)$_2$phen** at 612 nm is 12 nm red shifted compared to Ruphen (600 nm). This effect indicated a stabilized ^{3}MLCT state localized on the substituted phenanthroline. Interesting is the fact that the ^{1}MLCT of that compound exhibits no stabilization (see above).

Ru(tbp)$_4$phen emits at the same wavelength (613 nm) as **Ru(tbp)$_2$phen** but the emission of Ru((tFm)$_2$ph)$_2$phen at 652 nm deviates which again shows a stronger stabilization through the electron with-drawing substitution which is also observed in the ^{1}MLCT (see above).

In Rutpphz the emission is present due to the decay from a ^{3}MLCT state localized at the phenanthroline portion of the bridging ligand.[12,61]

The emission of **Ru(tbp)$_2$tpphz** is 8 nm red shifted compared to the emission of Rutpphz (measured under identical conditions) similar to the absorption of the ^{1}MLCT. In this case both states located at the substituted phenanthroline part are stabilized. As expected **Rutpphz(tbp)$_2$** emits at the same wavelength as Rutpphz.

Similar trends are observed for the brominated system, where the emission of RuBr$_2$tpphz is 21 nm red shifted compared to Rutpphz and the emission of RutpphzBr$_2$ is almost not shifted (4 nm).[24]

The emission of the dinuclear **Ru(tbp)$_2$tpphzRu** is very small in intensity which is similar to RutpphzRu and RuBr$_2$tpphzRu (where Ru = (tbbpy)$_2$Ru, tbbpy = 4,4'-di-*tert*.-butyl-2,2'-bipyridine and Br$_2$tpphz = 3,16-di-bromo-tetrapyrido[3,2-a:2',3'c:3'',2'',-h:2''',3'''-j]-phenazine).[62] We suggest that the emission in **Ru(tbp)$_2$tpphzRu** occurs solely from the substituted phenanthroline portion. This is based on the fact that only one emission is observed. Further the red shift of the emission of 60 nm compared to RutpphzRu shows that the stabilized phenanthroline portion is involved in this process.

In the case of RuBr$_2$tpphzRu similar effects are observed and the reason is described in detail.[62] Thereby stabilization caused through the brom-substitution concerns not only the ^{1}MLCT and ^{3}MLCT localized on the phenanthroline part but also the ^{3}MLCT localized on the phenazine part. By that the quenching of the ^{3}MLCT of the unsubstituted phenanthroline part of tpphz through the phenazine portion occurs very effective, which leads to the lack of the emission of the unsubstituted phenthroline part. Similar effects could occur in **Ru(tbp)$_2$tpphzRu** also.

Electrochemical investigation, however, indicates that the phenazine part in **Ru(tbp)$_2$tpphz** or **Rutpphz(tbp)$_2$** is not influenced as strong by the substitution as it is the case in RuBr$_2$tpphz or RutpphzBr$_2$ (see below and table 4). Consequently the phenazine centered state in the dinuclear complex might also be affected less by the phenyl substitution compared to the bromine substitution.

Another explanation for the single emission could be the recently for RutpphzRu described more complicated photophysical behavoiur.[63] There is shown that after the excitation of both Ru-moieties and the formation of two ^{3}MLCT states located on both phenathroline parts of tpphz deactivation of one of the states and simultaneous formation of a singly excited unit occurs.

Electrochemistry

The cyclic voltammograms and the square wave potentiometric measurements lead to redox potentials that are listed in Table 4 together with the potentials of some reference compounds.

In the comparison between Rutpphz versus bpy$_2$Rutpphz[23] Rutpphz shows negative shifted values of all potentials which might be due to the higher electron density in Rutpphz due to the *tert*.-butyl-groups on the bypyridyne-ligands.

In the comparison of Rutpphz versus RuBr$_2$tpphz or RutpphzBr$_2$ the latter two complexes exhibit positive shifted values for E_{ox} and E_{red}^I induced by the electron withdrawing effect of the bromines for RuBr$_2$tpphz and RutpphzBr$_2$.[24]

The redox potentials of the ruthenium centers of the here presented complexes vary just within experimental error (0.83 – 0.86 V). In contrast to the bromine-substitution the *tert*.-butyl-phenyl-substitution does not affect the oxidation potential of Ru^{II}/Ru^{III}.

Dalton Transactions Accepted Manuscript

Dalton Transactions RSCPublishing

PAPER

Table 4: electrochemical potentials *E* [V] of the complexes (vs. Fc/Fc^+) in ACN[a].

	E_{ox}	E_{red}^{I}	E_{red}^{II}	E_{red}^{III}	E_{red}^{IV}	E_{red}^{V}	E_{red}^{VI}
Ruphen[b]	0.78	-1.80	-1.99	-2.23			
Ru(tbp)$_2$phen[c]	0.81	-1.70	-1.98	-2.22	-2.58	-3.12	
Ru((tFm)$_2$ph)$_2$phen[d]	0.81	-1.69	-1.95	-2.21	-2.56		
bpy$_2$Rutpphz[e]	0.90	- 1.30	-1.76	-1.94	-2.16		
Rutpphz[f]	0.83	-1.39	-1.90	-2.10	-2.45[g]	-2.88[g]	-3.09
Rutpphz[h]	0.83	-1.39	-1.88	-2.05	-2.26[g]		
Rutpphz[i]		-1.44	-1.91	-2.13	-2.31[g]	-2.59[g]	
Rutpphz(tbp)$_2$[j]	0.83	-1.35	-1.90	-2.10	-2.41	-2.82	
Ru(tbp)$_2$tpphz[k]	0.86	-1.35	-1.86	-2.02	-2.26	-2.68	-3.06
RutpphzBr$_2$[h]	0.91	-1.25	-1.89	-2.06	-2.25		
RuBr$_2$tpphz[h]	0.89	-1.18	-1.87	-2.03	-2.18		
RutpphzRu[i]		-1.16	-1.88	-2.07	-2.31		
Ru(tbp)$_2$tpphzRu[c]	0.84	-1.18	-1.77	-1.93	-2.23	-2.49	-2.93
bpy$_2$RutpphzRubpy$_2$[e]	0.91	-1.14	-1.74	-1.94	-2.15		

[a] electrochemical measurements were carried out in anhydrous ACN with 0.1 M tetrabutylammonium hexafluorophosphate as supporting electrolyte; [b] from reference [64]; [c] $c_{complex}$ = 2 mM; [d] from reference [59]; [e] from reference [23]; Fc/Fc^+ = + 0.43 V vs. SCE in acetonitrile; [f] $c_{complex}$ = 0.5 mM; [g] deviation due to different setup; [h] from reference [24]; [i] from reference [6]; [j] $c_{complex}$ = 0.08 mM; [k] $c_{complex}$ = 0.25 mM.

The first reduction is assigned to be centered on the phenazine portion of the tpphz moiety. The *tert*.-butyl-phenyl-substitution does not influence this potential significantly. This observation is in contrast to the results obtained for the related bromine substituted complexes. There a pronounced influence of the substituents on this redox potential could be observed.[24]

The values of the first reduction potential are concentration dependent for the complexes Rutpphz, **Rutpphz(tbp)$_2$** and **Ru(tbp)$_2$tpphz** whereas the phenazine reduction band shows a more complex behavior. At low concentration a single signal can be observed whereas at higher concentration two signals appear at very similar potentials. (Rutpphz: E_{red}^{I} (0.5 mM) = -1,39 V; E_{red}^{I} (2 mM) = -1,37 V, shoulder -1.44 V. **Ru(tbp)$_2$tpphz**: E_{red}^{I} (0.25 mM) = -1,35 V; E_{red}^{I} (1 mM) = -1,38 V, shoulder -1.48 V. **Rutpphz(tbp)$_2$**: E_{red}^{I} (0.08 mM) = -1,35 V; E_{red}^{I} (0,5 mM) = -1,34 V, -1.47 V). MacDonnell observed similar effect for a Ruthenium complex containing a large aromatic system and suggested that dimerization of the complexes to be the reason for that effect.[65]

The second and third reductions occur probably on the peripheral tbbpy ligands analog to bpy$_2$Rutpphz.[23] Interesting is the indication of a positive shift when the bromine or *tert*.-butyl-phenyl substitution of the tpphz-moiety is located close to Ruthenium. When the substitution is located at the remote position no shift of E_{red}^{II} and E_{red}^{III} is noticeable.

Similar effect but more pronounced is observed for E_{red}^{IV}. The forth reduction potential for bpy$_2$Rutpphz is assigned to a second tpphz reduction[23] and more precise to the reduction of the phenanthroline part of tpphz which is bound to Ruthenium[24]. The value of E_{red}^{IV} of Rutpphz is similar to Rutpphz-complexes which exhibit a bromo- or *tert*.-butyl-phenyl-substitution at the remote position. But when the substitution is located at the close proximity to Ruthenium the values increase clearly. The reason for the easier reduction might be the electron withdrawing effect in the case of bromines and a delocalization of the electrons in the case of *tert*.-butyl-phenyl-substitution. Both substitutions induce a stabilization of the phenanthroline portion as already observed in the photophysics.

The redox potentials of the reference system **Ru(tbp)$_2$phen** are comparable with Ruphen[64] except the first reduction potential which is more positive. Ru((tFm)$_2$ph)$_2$phen[59] shows similar redox-behavior. This indicates that the first reduction occurs on the phenanthroline ligand and due to the stabilization through the phenyl-substitution the reduction is easier. Thereby it is indifferent if electron-withdrawing groups or electron-donating groups are localized on the phenyl-substituent.

The dimeric **Ru(tbp)$_2$tpphzRu** shows a positive shift of the E_{red}^{I} compared to the mononuclear compounds similar to bpy$_2$RutpphzRubpy$_2$ - bpy$_2$Rutpphz and Rutpphz – RutpphzRu couple (measured under identical conditions).[23] This occurs due to the introduction of a second positively charged metal center.[23] But also E_{red}^{II} and E_{red}^{III} are positively shifted in the case of **Ru(tbp)$_2$tpphzRu** compared with the monomeric species in contrast to the bpy$_2$RutpphzRubpy$_2$ - bpy$_2$Rutpphz and the Rutpphz – RutpphzRu couple (measured under identical conditions).

E_{red}^{IV} and E_{red}^{V} belong probably to the reduction of the substituted phenanthroline part and the unsubstituted phenanthroline part of tpphz respectively. This assignment may be drawn because the

Dalton Transactions Accepted Manuscript

monomeric species show comparable values of E_{red}^{IV} which are assigned to the reduction of the phenanthroline part of tpphz bound to Ruthenium.

Conclusion

The new synthesis route of the well soluble **tpphz(tbp)$_2$** presented here opens up a possibility of versatile derivatisation and application of the nearly insoluble tpphz scaffold. By changing the boronic acid in the Suzuki coupling reaction the substitution on the tpphz could be modified and thus lead to a different packing in the crystal. Based on the observed ordered packing of **tpphz(tbp)$_2$** in the solid state future applications in crystal engineering, liquid crystals are feasible. Therefor **tpphz(tbp)$_2$** might be an interesting compound for the research area of electron transport within organic devices[37,38] and liquid crystals.[66] As this ligand shows concentration dependency in the NMR-experiments it is likely that it arranges in solution in similar piles as in the crystal. The possible variation of the substitution opens a large variety of solubility and stability properties of the tpphz-core or the potential tpphz-pile.[38] A similar conjugated poly-heterocyclic molecule showed the aggregation in solution to liquid crystals.[66]

Further we have elucidated structural, photophysical and electrochemical properties of the here presented compounds. The complexes **Ru(tbp)$_2$tpphz** and **Rutpphz(tbp)$_2$** crystallize in a dimerized form which is usual for this type of complexes. Interesting is the finding that the latter exhibits beside the π-interaction of the tpphz-plane additional two CH-π-interactions of the phenyl-substituents which is similar to an interlocked "Fingerhakel".

Concentration dependent 1H-NMR investigation made a calculation of the dimerization constant (K_D) possible. The values for the complexes **Ru(tbp)$_2$tpphz** and **Rutpphz(tbp)$_2$** are very different whereas the latter shows a much higher value for this constant. We suppose the reason for that are the additional CH-π-interactions of the phenyl-substituents which we observed in the solid state. This effect could potentially be used to tune the photocatalytic activity with supramolecular additives as recently described for Rutpphz based photocatalyst.[56]

In the photophysics the two new regioisomeric complexes **Ru(tbp)$_2$tpphz** and **Rutpphz(tbp)$_2$** display a pronounced difference of the band at 350 nm which can be assigned to the *tert*.-butyl-phenyl-substitution of the ligand. For the complex **Ru(tbp)$_2$tpphz** a slight red shift in the ^{1}MLCT indicates a stabilization of the phenantroline portion of the tpphz induced by the substitution. The emission indicates also a stabilization of the ^{3}MLCT. For the model complex **Ru(tbp)$_2$phen** only the ^{3}MLCT seems to be stabilized.

The electrochemical investigation of **Ru(tbp)$_2$tpphz**, **Rutpphz(tbp)$_2$**, **Ru(tbp)$_2$phen** and **Ru(tbp)$_2$tpphzRu** display an easier reduction of the *tert*.-butyl-phenyl-substituted phenanthroline (part) which again shows the stabilization induced by the substitution. Interesting is the fact that the phenazine reduction is not influenced by the substitution contrary to $RuBr_2$tpphz and $RutpphzBr_2$. This effect might lead to a better electron transport along the bridge in a photo catalyst.

Experimental Section

In all reactions that were run under argon standard Schlenk techniques are used. 1,10-phenanthrolin-mono-hydrat, 4-*tert*.-butyl-phenyl-boronic acid, bromine, NH4PF6 and all other materials were of commercial grade and used without further purification. 3,8-Dibromo-1,10-phenanthroline-5,6-dione[24,59], $[(tbbpy)_2RuCl_2]$[67,68] and 1,10-phenanthroline-5,6-diamine ($phen(NH_2)_2$)[69,70] were prepared according to literature methods.

^{1}H NMR and ^{13}C NMR spectra were recorded at ambient temperature on a Bruker AVANCE 400 (400 MHz) and a Bruker AVANCE 500 (500 MHz) spectrometer. All spectra were referenced to deuterated solvent as an internal standard.

Chemical Ionization mass spectrometry (CI) was performed on a Finnigan MAT SSQ-7000 (1994) instrument at the University Ulm. High-resolution mass spectrometry (HRMS) was performed using a Fourier Transform Ion Cyclotron Resonance (FT-ICR) mass spectrometer solariX (Bruker Daltonik GmbH, Bremen, Germany) equipped with a 7.0 T superconducting magnet and interfaced to an Apollo II Dual ESI/MALDI source, which can be switched from ESI to MALDI operation almost instantaneously. In MALDI operation mode dithranol, DCTB or DHB were used as the matrix. In ESI operation mode acetonitrile was used as the solvent.

UV/Vis spectra (accuracy ± 2 nm) were obtained by using a JASCO Spectrometer V-670 at ambient temperature. Emission spectra were measured at ambient temperature by using a JASCO Spectrafluorometer FP-8500. Quartz cells with a 10 mm path-length were used for recording UV/Vis and emission spectra. All experiments were repeated 3 times.

The microwave-assisted reactions were carried out by using the Microwave Laboratory System Start 1500 from MLS GmbH.

Elemental analyses were performed on a vario MICRO cube.

Electrochemical data were obtained by cyclic voltammetry and square wave voltammetry using a conventional single-compartment three-electrode cell arrangement in combination with an advanced Potentiostat/Galvanostat PARSTAT 2273 from PRINCETON APPLIED RESEARCH. As working electrode: glassy carbon, auxiliary electrode and reference electrode: Platin-wire respectively. The measurements were carried out in anhydrous and argon purged ACN with 0.1 M tetrabutylammonium hexafluorophosphate as supporting electrolyte. At the end of each experiment, ferrocene was added as an internal standard and the observed potential was set to 0 V.

This paper contains nine crystal structures, CCDC-1015495-1043862, 1015495, and 1015496. Data for these structures can be obtained free of charge from The Cambridge Crystallographic Data Centre via www.ccdc.cam.ac.uk/data_request/cif. Crystals suitable for X-ray analysis were mounted using a MicroLoop and Fomblin oil. X-ray diffraction intensity data were measured at 180 K or 150 K on a SuperNova (Dual Source) diffractometer using Mo or Cu radiation, equipped with an ATLAS detector, from Agilent Technologies. The structures were solved by direct methods (SHELXS) and refined by full-matrix least squares techniques against F_o^2 (SHELXL 2013).[71] The Platon Squeeze procedure was applied for some structures to remove diffuse solvent molecules.[72] Hydrogen atoms were included at calculated positions with fixed thermal parameters. All non-hydrogen atoms were refined anisotropically.

Synthesis

3,8-Dibromo-2,2-Dimethyl-1,3-dioxolo[4,5-f]-1,10-phenanthrolin (phenBr_2O_2X)

For this synthesis a slightly modified literature procedure was used[25]. 3,8-Dibromo-1,10-phenanthroline-5,6-dione (0.5 g, 1.36 mmol) and 2-nitropropane (12.1 g, 136 mmol) were suspended in acetonitrile/water (15 mL/15 mL) and degassed. Afterwards a degassed, aqueous solution of sodium carbonate (2 M, 0.7 mL, 1 eqiv.) was added. The reaction mixture was then heated to reflux for 40 minutes. After cooling to room temperature the product was extracted with dichloromethane. The combined organic extracts were dried over magnesium sulfate, filtered and dried using the rotary evaporator. The product is a lime green solid.

Dalton Transactions Accepted Manuscript

Dalton Transactions RSCPublishing

PAPER

Yield = 72 % (3.2 g); **M** ($C_{15}H_{10}Br_2N_2O_2$) = 410.06 g mol^{-1}; **Anal. Calcd** for $C_{15}H_{10}Br_2N_2O_2$: C = 43.94, H = 2.46, N = 6.83; found: C = 42.46, H = 2.53, N = 6.95; **MS** (CI): m/z = 329 $[M-Br]^+$, 411 $[M+H]^+$, 439 $[M+C_2H_5]^+$; **^{1}H-NMR** (400 MHz, $CDCl_3$, 300 K): δ = 9.04 (d, J = 2.3 Hz, 2H), 8.40 (d, J = 2.4 Hz, 2H), 1.60 (s, 6 H) ppm. **^{13}C-NMR** (100 MHz, $CDCl_3$, 300 K): δ = 26.17, 119.21, 120.34, 121.97, 130.03, 136.67, 140.33, 149.23 ppm. **Crystals** suitable for X-ray analysis were obtained from $CHCl_3$ and diethyl ether. Crystal data for phenBr_2O_2X: C_{15} H_{10} Br_2 N_2 O_2, M_r = 410.07 g mol^{-1}, yellow fragment, crystal size 0.38 x 0.14 x 0.04 mm^3, triclinic, space group P -1, a = 6.9502(7) Å, b = 10.2517(9) Å, c = 10.6485(9) Å, α = 82.560(7)°, β = 78.404(8)°, γ = 75.662(8), V = 717.54(12) Å^3, T = 150(2) K, Z = 2, $\rho_{calcd.}$ = 1.898 Mg/m3, μ (Mo-Kα) = 5.653 mm^{-1}, F(000) = 400, altogether 5644 reflexes up to h(-8/8), k(-12/10), l(-13/13) measured in the range of 3.441° ≤ Θ ≤ 26.372° , completeness Θ_{max} = 99.7 %, 2927 independent reflections, R_{int} = 0.0317, 2483 reflections with Fo > 4 σ(Fo), 192 parameters, 0 restraints, $R1_{obs}$ = 0.0394, $wR2_{obs}$ = 0.1080, $R1_{all}$ = 0.0474, $wR2_{all}$ = 0.1148, GOOF = 1.108, largest difference peak and hole: 1.027/-0.758 e·Å^{-3}. CCDC 1034411 contains the supplementary crystallographic data for this paper. **TLC**: (Silica, $CHCl_3$) R_f = 0.27, (Silica, Ethylacetate) R_f = 0.7.

3,8-Bis(4-*tert*.-butyl-phenyl)-2,2-Dimethyl-1,3-dioxolo[4,5-f]-1,10-phenanthrolin (phen(tbp)$_2$O$_2$X)

For this synthesis a slightly modified literature procedure was used[59]. The catalytic reaction was performed under inert conditions. phenBr_2O_2X (0.900 g, 2.19 mmol), 4-tetrabutylphenylboronic acid (0.940 g, 5.28 mmol), NaOH (3.65 g, 91.2 mmol), S-Phos (0.184 g, 0.448 mmol) were placed into a Schlenk tube. Thereafter, freshly distilled tetrahydrofuran (653 mL) and deoxygenated water (47 mL) were added. The mixture was degassed with argon for 30 minutes. After addition of $Pd_2(dba)_3$ (0.206 g, 0.225 mmol) the yellow reaction mixture was heated at reflux under argon for 3 d. The suspension was then cooled to room temperature, taken up into water and extracted with chloroform. The solvent of the combined organic layers was removed and the crude product was cleaned by column chromatography (silica and chloroform) and recrystallization from acetone. **Yield** = 74 % (0.844 g); **M** ($C_{35}H_{36}N_2O_2$) = 516.67 g mol^{-1}; **Anal. Calcd** for $C_{35}H_{36}N_2O_2$: C = 81.36, H = 7.02, N = 5.42; found: C = 79.74, H = 6.87, N = 5.17; **MS** (CI): m/z = 461 [M-*tert*.-butyl+2H]$^+$, 501 $[M-CH_3]^+$, 516 $[M]^+$; **^{1}H-NMR** (400 MHz, $CDCl_3$, 300 K): δ = 9.34 (d, J = 2.3 Hz, 2H), 8.41 (d, J = 2.3 Hz, 2H), 7.80 – 7.71 (m, 4H), 7.60 – 7.54 (m, 4H), 1.39 (s, 18H) ppm. **^{13}C-NMR** (100 MHz, $CDCl_3$, 300 K): δ = 26.22, 31.43, 34.80, 118.24, 120.90, 125.06, 126.27, 127.35, 134.81, 135.19, 136.93, 141.23, 147.26, 151.72 ppm. **Crystals** suitable for X-ray analysis were obtained from chloroform and diethyl ether. Crystal data for phen(tbp)$_2$O$_2$X: C_{36} H_{37} Cl_3 N_2 O_2, M_r = 636.02 g mol^{-1}, yellow fragment, crystal size 0.34 x 0.17 x 0.15 mm^3, triclinic, space group P -1, a = 10.9557(7) Å, b = 11.8569(7) Å, c = 14.1102(9) Å, α = 104.299(5)°, β = 115.158(8)°, γ = 95.094(5), V = 1642.82(19) Å^3, T = 150(2) K, Z = 2, $\rho_{calcd.}$ = 1.286 Mg/m3, μ (Cu-Kα) = 2.792 mm^{-1}, F(000) = 668, altogether 11349 reflexes up to h(-13/12), k(-14/14), l(-17/17) measured in the range of 7.593° ≤ Θ ≤ 73.963° , completeness Θ_{max} = 99.5 %, 6421 independent reflections, R_{int} =0.0188, 5968 reflections with Fo > 4 σ(Fo), 420 parameters, 0 restraints, $R1_{obs}$ = 0.0561, $wR2_{obs}$ = 0.1450, $R1_{all}$ = 0.0588, $wR2_{all}$ = 0.1474, GOOF = 1.028, largest difference peak and hole: 1.322/-0.537 e·Å^{-3}. CCDC 1034410 contains the supplementary crystallographic data for this paper. **TLC**: (Silica, Ethylacetate) R_f = 0.1 (emitting yellow).

3,8-Bis(4-*tert*.-butyl-phenyl)-1,10-phenanthrolin (phen(tbp)$_2$)

For this synthesis a slightly modified literature procedure was used[49]. The reaction was achieved under inert conditions. 3,8-dibromphenathroline (0.61 mmol, 206 mg), (p-tetrabutyl-phenyl)boronic acid (2.6 mmol, 462 mg), sodium carbonate (0.04 mmol, 4.24 g) and palladium-tetraphenylphosphin (0.06 mmol, 0.07 mg) were suspended in a degassed toluol/water mixture (3/1, 80 mL) and heated at reflux for 5 days. The solution was extracted with chloroform and water and the combined organic layers were drayed with $MgSO_4$. After the solvent was evaporated the product was purified with column chromatography (silica, chloroform) and recrystallization from chloroform ethyl acetate. Received was a white powder. **Yield** = 60 % (0.161 g); **M** ($C_{32}H_{32}N_2$) = 444.61 g mol^{-1}; **Anal. Calcd** for $C_{32}H_{32}N_2$: C = 86.44, H = 7.25, N = 6.30; found: C = 84.15, H = 6.84, N = 5.84; **MS** (CI): m/z = 389 [M-*tert*.-butyl+2H]$^+$, 429 $[M-CH_3]^+$, 444 $[M]^+$; **^{1}H-NMR** (400 MHz, $CDCl_3$, 300 K): δ = 9.45 (d, J = 2.3 Hz, 2H), 8.38 (d, J = 2.3 Hz, 2H), 7.87 (s, 2H), 7.79 – 7.70 (m, 4H), 7.63 – 7.54 (m, 4H), 1.40 (s, 9H). **^{13}C-NMR** (100 MHz, $CDCl_3$, 300 K): δ = 31.44, 34.84, 126.41, 127.23, 127.33, 128.65, 133.50, 134.48, 135.84, 144.20, 149.40, 151.89 ppm. **Crystals** suitable for X-ray analysis were obtained from chloroform/diethyl ether. Crystal data for phen(tbp)$_2$: C_{32} H_{32} N_2, M_r = 444.59 g mol^{-1}, colourless fragment, crystal size 0.24 x 0.09 x 0.04 mm^3, monoclinic, space group P 2_1/n, a = 16.2831(12) Å, b = 9.4620(5) Å, c = 17.5232(11) Å, β = 115.158(8)°, V = 2443.7(3) Å^3, T = 180(2) K, Z = 4, $\rho_{calcd.}$ = 1.208 Mg/m3, μ (Cu-Kα) = 0.531 mm^{-1}, F(000) = 952, altogether 10148 reflexes up to h(-20/16), k(-11/11), l(-21/21) measured in the range of 7.604° ≤ Θ ≤ 74.114° , completeness Θ_{max} = 99.6 %, 4800 independent reflections, R_{int} = 0.0306, 3180 reflections with Fo > 4 σ(Fo), 335 parameters, 0 restraints, $R1_{obs}$ = 0.0670, $wR2_{obs}$ = 0.1870, $R1_{all}$ = 0.0980, $wR2_{all}$ = 0.2194, GOOF = 1.037, largest difference peak and hole: 0.486/-0.231 e·Å^{-3}. CCDC 1034409 contains the supplementary crystallographic data for this paper. **TLC**: (Silica, Ethylacetate) R_f = 0.1 (emitting blue).

3,8-Bis(4-*tert*.-butyl-phenyl)-1,10-phenanthrolin-5,6-dione (phen(tbp)$_2$O$_2$)

For this synthesis a slightly modified literature procedure was used[25]. The protected phen(tbp)$_2$O$_2$X (1.56 g, 3.02 mmol) was dissolved in a mixture of water (25 mL) and clear trifluoracetic acid (50 mL). The mixture was stirred at 50 °C for 21 h. Afterwards the solvent was evaporated under reduced pressure and the residue was extracted with chloroform whereas pH of the water phase was tuned to pH 9 by adding sodium hydrogen carbonate. The side product 3,8-Bis(4-*tert*.-butyl-phenyl)-1,10-phenanthrolin-5,6-diol (phen(tbp)$_2$(OH)$_2$) precipitate under these conditions and stays between the phases. It can be filtered of after the extraction. The organic layers were dried over MgSO4 and filtered. For purification of the orange solid column chromatography was used (silica and

Dalton Transactions Accepted Manuscript

dichloromethane, whereas a gradient was driven from 100% DCM to 97%/3% DCM/MeOH). **Yield** = 51 % (0.732 g); **M** ($C_{32}H_{30}N_2O_2$) = 474.23 g mol^{-1}; **Anal. Calcd** for $C_{32}H_{30}N_2O_2$: C = 80.98, H = 6.37, N = 5.90; found: C = 80.61, H = 7.07, N = 5.67;
MS (CI): m/z = 419 [M-*tert*.-butyl+2H]$^+$, 475 [M+H]$^+$, 503 [M+C_2H_5]$^+$; **^{1}H-NMR** (400 MHz, $CDCl_3$, 300 K): δ = 9.34 (d, J = 2.4 Hz, 2H), 8.67 (d, J = 2.4 Hz, 2H), 7.75 – 7.64 (m, 4H), 7.63 – 7.53 (m, 4H), 1.39 (s, 18H) ppm. **^{13}C-NMR** (100 MHz, $CDCl_3$, 300 K): δ = 31.37, 34.93, 126.59, 126.95, 127.78, 132.60, 134.64, 138.25, 151.27, 153.01, 154.64, 179.20 ppm. **Crystals** suitable for X-ray analysis were obtained from acetonitrile and diethyl ether. Crystal data for phen(tbp)$_2$O$_2$: C_{32} H_{30} N_2 O_2, M_r = 474.58 g mol^{-1}, yellow fragment, crystal size 0.29 x 0.08 x 0.05 mm^3, triclinic, space group *P* -1, a = 6.3897(4) Å, b = 10.1543(7) Å, c = 19.0511(13) Å, α = 97.594(6)°, β = 91.675(5)°, γ = 92.920(6), V = 1222.85(14) Å^3, T = 150(2) K, Z = 2, $\rho_{calcd.}$ = 1.289 Mg/m3, μ (Cu-Kα) = 0.630 mm^{-1}, F(000) = 504, altogether 14141 reflexes up to h(-7/7), k(-12/10), l(-23/23) measured in the range of 7.412° ≤ Θ ≤ 73.739° , completeness Θ_{max} = 99.7 %, 4802 independent reflections, R_{int} = 0.0317, 3622 reflections with Fo > 4 σ(Fo), 325 parameters, 0 restraints, $R1_{obs}$ = 0.0467, $wR2_{obs}$ = 0.1165, $R1_{all}$ = 0.0653, $wR2_{all}$ = 0.1285, GOOF = 1.079, largest difference peak and hole: 0.241/-0.192 e·Å^{-3}. CCDC 1034412 contains the supplementary crystallographic data for this paper. **TLC**: (Silica, DCM/MeOH = 95.5/4.5) R_f = 0.44.
Diol: **M** ($C_{32}H_{32}N_2O_2$) = 476.61 g mol^{-1}; **Anal. Calcd** for $C_{32}H_{32}N_2O_2$: C = 80.64, H = 6.77, N = 5.88; found: C = 80.84, H = 7.05, N = 5.71; **MS** (CI): m/z = 421 [M-*tert*.-butyl+2H]$^+$, 461 [M-OH+2H]$^+$, 477 [M+H]$^+$, 505 [M+CH_3CH_2]$^+$, 515 [M+K]$^+$; **^{1}H-NMR** (400 MHz, $CDCl_3$ + 1 drop F_3C-COOD, 300 K): δ = 9.00 (d, J = 2.0 Hz, 2H), 8.75 (d, J = 2.0 Hz, 2H), 7.53 (s, 8H), 1.38 (s, 18H).

3,16-Di(4-*tert*.-butyl-phenyl)-tetrapyridophenazine (tpphz(tbp)$_2$)

For this synthesis a slightly modified literature procedure was used[24]. A mixture of phen(tbp)$_2$O$_2$ (0.606 g, 1.28 mmol) and 1,10-phenanthroline-5,6-diamine (0.362 g, 1.72 mmol) in 120 mL dry methanol was refluxed for two days under argon atmosphere. After cooling the reaction mixture to room temperature the solvent was removed. To purify the crude product column chromatography was used (silica and dichloromethane, whereas a gradient was driven from 100% DCM to 97%/3% DCM/MeOH) and recrystallization from chloroform and ethanol/water. As product a light yellow precipitate was obtained. **Yield** = 88 % (0.768 g); **M** ($C_{44}H_{36}N_6$) = 648.80 g mol^{-1}; **Anal. Calcd** for $C_{44}H_{36}N_6$ + H_2O: C = 79.25, H = 5.74, N = 12.60; found: C = 79.14, H = 5.72, N = 12.79; **MS** (MALDI-HRMS): m/z calc. for $C_{44}H_{36}N_6$ + H: 649.30742; found = [M+H]$^+$ 649.30740 (0.03 ppm); m/z calc. for $C_{44}H_{36}N_6$ + Na: 671.28991 ; found = [M+Na]$^+$ 671.28820 (2.55 ppm); m/z calc. for 2 $C_{44}H_{36}N_6$ + Na: 1319.59006; found = [2M+Na]$^+$ 1319.59745 (5.6 ppm); **^{1}H-NMR** (400 MHz, $CDCl_3$, 300 K, c = 1.03 mM): δ = 9.83 (d, J = 2.3 Hz, 2H), 9.71 (dd, J = 8.1, 1.7 Hz, 2H), 9.56 (d, J = 2.3 Hz, 2H), 9.34 (dd, J = 4.4, 1.7 Hz, 2H), 7.89 (d, J = 8.3 Hz, 4H), 7.85 (dd, J = 8.1, 4.4 Hz, 2H), 7.70 (d, J = 8.3 Hz, 4H), 1.47 (s, 18H) ppm. **^{13}C-NMR** (100 MHz, $CDCl_3$ + droplet of TFA-d_1, 300 K): δ = 31.29, 35.17, 127.29, 127.61, 127.68, 128.21, 128.70, 131.26, 135.72, 138.28, 139.50, 139.75, 140.03, 140.57, 140.13, 148.18, 149.70, 154.79 ppm. **Crystals** suitable for X-ray analysis were obtained from dichloromethane. Crystal data for tpphz(tbp)$_2$: C_{47} H_{42} Cl_6 N_6, M_r = 903.56 g mol^{-1}, colourless fragment, crystal size 0.14 x 0.09 x 0.04 mm^3, triclinic, space group *P* -1, a = 7.6741(4) Å, b = 15.7010(6) Å, c = 19.5176(8) Å, α = 73.800(4)°, β = 88.093(4)°, γ = 86.939(4), V = 2254.68(18) Å^3, T = 180(2) K, Z = 2, $\rho_{calcd.}$ = 1.331 Mg/m^3, μ (Cu-Kα) = 3.790 mm^{-1}, F(000) = 936, altogether 22502 reflexes up to h(-9/9), k(-14/19), l(-23/24) measured in the range of 7.397° ≤ Θ ≤ 74.491° , completeness Θ_{max} = 99.7 %, 9194 independent reflections, R_{int} = 0.0424, 6656 reflections with Fo > 4 σ(Fo), 542 parameters, 0 restraints, $R1_{obs}$ = 0.0730, $wR2_{obs}$ = 0.2191, $R1_{all}$ = 0.0945, $wR2_{all}$ = 0.2337, GOOF = 1.114, largest difference peak and hole: 1.090/-0.514 e·Å^{-3}. CCDC 1034413 contains the supplementary crystallographic data for this paper.
Three molecules of dichloromethane were found in the crystal lattice, but refinement was only carried out for two of them. A residual electron density maximum (Uij(Q1) = 2.06) close to the third solvent molecule indicated disorder, which could not be included in a meaningful way. Furthermore, restraints for the respective solvent molecule had to be applied to preserve its geometry during the refinement. Therefore, the Platon Squeeze procedure was applied in order to remove the disordered molecule from the data and receive moderate refinement values. All crystal parameters were calculated with the full sum fomula including all solvent molecules.
TLC: (Silica, DCM/MeOH = 93%/7%) R_f = 0.06 (green emitting)

Ru(tbp)$_2$tpphz, Rutpphz(tbp)$_2$ as PF_6-salts

For this synthesis a slightly modified literature procedure was used[24]. A purple solution of [(tbbpy)$_2$RuCl$_2$] (50 mg, 0.070 mmol) in ethanol/water (20mL/12mL) was added dropwise to a boiling mixture of a twofold excess of tpphz(tbp)$_2$ (90.8 mg, 0.140 mmol) dissolved in 40 mL ethanol. The reaction mixture was stirred and heated to reflux through the microwave irradiation (150 W) for 1.5 h. The solvent was distilled off until 15 mL of solution remained. Then the unconverted tpphz(tbp)$_2$ was filtered off from the colored solution and washed with ethanol/water mixture (50/50). The ethanol of the combined filtrates was removed. The complexes were extracted with dichloromethane and water whereas a tenfold excess of sodium benzosulfonate was added for the product exhibits benzosulfonate as counterion. To separate the isomers from each other column chromatography was used (silica and acetonitrile, whereas a gradient was driven from 100 % acetonitrile to 87/17% acetonitrile/0.05 M sodium-benzosulfonate water solution, only small amounts can be separated in one go (ca. 40 mg). To get rid of sodium-benzosufonate an extraction in water and dichloromethane was achieved several times followed by precipitation with hundredfold excess of NH_4PF_6 out of a water/ethanol/DCM solution whereas DCM needs to be evaporated for the product to precipitate. The product was further purified with the aid of recrystallization from acetone/water. As a side product the dinuclear Ruthenium-complex of the bridging ligand was obtained in small amounts. **Yield** = 26 % (isomer 1: 118 mg , isomer 2: 65.5 mg); **M** ($C_{80}H_{84}F_{12}N_{10}P_2Ru$) = 1576.59 g mol^{-1};

Characterization of Ru(tbp)$_2$tpphz:

Anal. Calcd for isomer (1) $C_{80}H_{84}F_{12}N_{10}P_2Ru$: C = 60.95, H = 5.37, N = 8.88; found: C = 61.17, H = 5.59, N = 8.64; **MS** (ESI-HRMS): m/z calc. for $C_{80}H_{84}F_{12}N_{10}P_2Ru$ – 2 (PF_6): 643.29674; found = [M+H]$^+$ 643.29595 (1.23 ppm); m/z calc. for $C_{80}H_{84}F_{12}N_{10}P_2Ru$ – (PF_6): 1431.55657; found = [M-(PF_6)]$^+$ 1431.55895 (1.66 ppm); **^{1}H NMR** (400 MHz, CD_3CN, 300 K, c = 1.92 mM) δ = 9.84 (dd, J = 8.1, 1.7 Hz, 2H), 9.65 (d, J = 1.5 Hz, 2H), 8.67 (s, 2H), 8.64 (d, J = 1.9 Hz, 2H), 8.56 (d, J = 1.9 Hz, 2H), 8.16 (d, J = 1.9 Hz, 2H), 8.14 (s, 1H), 7.93 (d, J = 6.0 Hz, sH), 7.67 – 7.77 (m, 10H), 7.61 (dd, J = 6.0, 2.1 Hz, 2H), 7.36 (dd, J = 6.1, 1.9 Hz, 2H), 1.54 (s, 18H), 1.44 (s, 18H), 1.36 (s, 18H). **^{13}C-NMR** (100 MHz, $CDCl_3$, 300 K, conz.-independent): δ = 30.39, 30.53, 31.39, 35.49, 36.13, 36.44, 122.42, 122.44, 125.07, 125.42, 125.90, 126.89, 127.57, 128.39, 129.36, 130.12, 133.11, 134.74, 139.39, 139.69, 141.00, 148.06, 149.15, 151.90, 152.62, 152.95, 154.36, 154.71, 157.12, 158.61, 163.07, 163.76 ppm. **Crystals** suitable for X-ray analysis were obtained

Dalton Transactions Accepted Manuscript

from dichlormethane. Crystal data for Ru(tbp)$_2$tpphz: C_{96} H_{108} F_{12} N_{18} P_2 Ru, M_r = 1905.01 g mol^{-1}, red fragment, crystal size 0.21 x 0.14 x 0.09 mm^3, monoclinic, space group *C* 2/c, a = 51.8116(7) Å, b = 15.1574(2) Å, c = 25.2431(3) Å, β = 91.5900(10)° V = 19816.5(4) Å^3, T = 180(2) K, Z = 8, $\rho_{calcd.}$ = 1.277 Mg/m^3, μ (Cu-Kα) = 2.222 mm^{-1}, F(000) = 7936, altogether 56735 reflexes up to h(-47/62), k(-18/18), l(-31/30) measured in the range of 7.452° ≤ Θ ≤ 72.564° , completeness Θ_{max} = 99.3 %, 19053 independent reflections, R_{int} = 0.0289, 13808 reflections with Fo > 4 σ(Fo), 991 parameters, 6 restraints, $R1_{obs}$ = 0.0495, $wR2_{obs}$ = 0.1341, $R1_{all}$ = 0.0675, $wR2_{all}$ = 0.1472, GOOF = 0.780, largest difference peak and hole: 0.725/-0.588 e·Å^{-3}. CCDC 1015495 contains the supplementary crystallographic data for this paper. Altogether, eight molecules of acetonitrile were found per formula unit within the electron density map. However, a stable refinement could only be achieved using strict restraints on seven solvent molecules to preserve their geometry. Therefore, the Platon Squeeze procedure was applied to remove all but one molecules of acetonitrile from the data in order to get a stable refinement. All crystal parameters were calculated with the full sum fomula including all solvent molecules.

Characterization of Rutpphz(tbp)$_2$:

Anal. Calcd for isomer (2) $C_{80}H_{84}F_{12}N_{10}P_2Ru$ + 2 H_2O: C = 59.58, H = 5.50, N = 8.69; found: C = 59.99, H = 5.67, N = 8.45; **MS** (ESI-HRMS): m/z calc. for $C_{80}H_{84}F_{12}N_{10}P_2Ru$ – 2 (PF_6): 643.29674; found = $[M+H]^+$ 643.29656 (0.30 ppm); **^{1}H NMR** (400 MHz, CD_3CN, 300 K, c = 1.92 mM) δ = 9.76 (s, 2H), 9.39 (d, *J* = 7.9 Hz, 2H), 8.66 (s, 2H), 8.61 (d, *J* = 1.7 Hz, 2H), 8.57 (d, *J* = 1.5 Hz, 2H), 8.22 – 8.16 (m, 2H), 8.00 (s, 2H), 7.91 (d, *J* = 8.0 Hz, 4H), 7.80 (d, *J* = 5.9 Hz, 2H), 7.68 (d, *J* = 8.2 Hz, 4H), 7.65 – 7.57 (m, 2H), 7.54 (dd, *J* = 6.0, 2.0 Hz, 2H), 7.38 (d, *J* = 5.6 Hz, 2H), 1.50 (s, 18H), 1.46 (s, 18H), 1.36 (s, 18H). **^{13}C-NMR** (100 MHz, $CDCl_3$, 300 K, conz.-independent): δ = 163.73, 163.43, 158.13, 157.60, 154.57, 153.53, 153.37, 152.16, 151.31, 150.84, 146.57, 141.41, 139.26, 136.63, 134.11, 134.05, 130.25, 130.09, 127.99, 127.46, 127.31, 126.49, 125.90, 125.65, 122.50, 122.39, 36.38, 36.26, 35.44, 31.60, 30.53, 30.45 ppm. **Crystals** suitable for X-ray analysis were obtained from acetonitrile and diethyl ether. Crystal data for Rutpphz(tbp)$_2$: $C_{85.50}$ H_{95} Cl_{11} F_{12} N_{10} P_2, M_r = 2043.67 g mol^{-1}, tetragonal prism, crystal size 0.12 x 0.10 x 0.06 mm^3, monoclinic, space group *C* 2/c, a = 45.6046(9) Å, b = 22.1737(4) Å, c = 21.5480(6) Å, β = 116.956(3)°, V = 19422.5(9) Å^3, T = 150(2) K, Z = 8, $\rho_{calcd.}$ = 1.398 Mg/m^3, μ (Mo-Kα) = 0.567 mm^{-1}, F(000) = 8376, altogether 62965 reflexes up to h(-56/56), k(-27/26), l(-26/24) measured in the range of 3.408° ≤ Θ ≤ 26.372° , completeness Θ_{max} = 99.7 %, 19815 independent reflections, R_{int} = 0.0580, 14046 reflections with Fo > 4 σ(Fo), 1037 parameters, 0 restraints, $R1_{obs}$ = 0.0531, $wR2_{obs}$ = 0.1383, $R1_{all}$ = 0.0793, $wR2_{all}$ = 0.1510, GOOF = 0.985, largest difference peak and hole: 0.608/-0.496 e·Å^{-3}. CCDC 1015496 contains the supplementary crystallographic data for this paper. Four and a half molecules of dichloromethane (the half with the carbon atom presumably located within a C^2 axis) were recognized within the electron density map, but only two of them could be refined with minor disorder to achieve a stable refinement. Careful analysis of the Platon Squeeze calculations on the residual void volumina and electron counts at different refinement steps, lead to the conclusion that there are three and a half more molecules of dichloromethane (the half corresponding to the aforementioned C^2 symmetry) per formula unit in the unit cell, which could not be refined within their comparatively large voids due to disorder. All crystal parameters were calculated with the full sum fomula including all solvent molecules.

Ru(tbp)$_2$tpphzRu as PF_6-salt

For this synthesis a slightly modified literature procedure was used[23]. The ligand tpphz(tbp)$_2$ (50 mg, 0.077 mmol) was dissolved with [(tbbpy)$_2$RuCl$_2$] (272 mg, 0.385 mmol) in a ethanol/water mixture (3/2, 50 mL). The solution was heated to reflux for 2 days. The solvent was evaporated and the product was purified with column chromatography (silica and acetone, whereas a gradient was driven from 100 % acetone to 75%/25% acetone/water whereas the later contained 1%$_{vol}$ saturated KNO_3). The last fraction was collected and acetone was evaporated until water with a red precipitate remained. The Precipitate was filtered off and dissolved in an ethanol/water mixture. Afterwards NH_4PF_6 (125 mg, 0.77 mmol) dissolved in 1 mL water was added to the solution. Ethanol was evaporated of the mixture and the product was collected. For further purification a recrystallization from ACN/diethyl ether was achieved. **Yield** = 66 % (135 mg); **M** ($C_{44}H_{36}N_6$) = 2504.38 g mol^{-1}; **Anal. Calcd** for $C_{116}H_{132}F_{24}N_{14}P_4Ru_2$ + H_2O: C = 55.24, H = 5.33, N = 7.77; found: C = 54.92, H = 5.32, N = 8.08; **MS** (ESI-HRMS): m/z calc. for $C_{116}H_{132}F_{24}N_{14}P_4Ru_2$ – 4 (PF_6): 481.22164; found = $[M-4(PF_6)]^{4+}$ 481.22210 (0.96 ppm); **^{1}H-NMR** (400 MHz, CD_3CN, 300 K): δ = 10.10 (m, *J* = 8.4, 1.3 Hz, 4H, c and c'), 8.61 (m, *J* = 2.1 Hz, 2H), 8.57 (m, *J* = 1.7 Hz, 2H), 8.53 (s, 4H), 8.27 (dd, *J* = 5.4, 1.2 Hz, 2H, a), 8.15 (dd, *J* = 1.8, 1.0 Hz, 2H, a'), 8.03 (dd, *J* = 8.2, 5.4 Hz, 2H, b), 7.88 (dd, *J* = 6.0, 3.0 Hz, 2H), 7.84 (dd, *J* = 6.1, 1.8 Hz, 2H), 7.76 – 7.72 (m, 2H), 7.70 (d, *J* = 8.5 Hz, 4H), 7.66 – 7.56 (m, 8H), 7.52 (dd, *J* = 6.1, 2.0 Hz, 2H), 7.32 – 7.22 (m, 4H), 1.50 (d, *J* = 0.7 Hz, 18H), 1.48 (s, 18H), 1.37 (dd, *J* = 3.9, 2.1 Hz, 54H). **^{13}C-NMR** (100 MHz, $CDCl_3$, 300 K): δ = 30.36, 30.45, 30.47, 31.30, 35.41, 36.20, 36.21, 36.32, 36.42, 122.49, 122.58, 122.80, 125.44, 125.55, 125.64, 127.46, 128.32, 128.50, 130.58, 130.96, 131.11, 133.19, 134.92, 140.68, 141.52, 141.78, 149.91, 149.93, 151.66, 151.68, 152.03, 152.44, 152.46, 152.52, 152.55, 152.64, 152.82, 154.36, 155.17, 157.60, 157.71, 157.98, 158.38, 163.55, 163.58, 163.72, 163.89 ppm. **Crystals** suitable for X-ray analysis were obtained from acetonitrile/methyl-*tert*.-butyl-ether. Crystal data for Ru(tbp)$_2$tpphzRu: $C_{143.50}$ H_{198} F_{24} N_{14} $O_{5.50}$ P_4 Ru_2, M_r = 2989.17 g mol^{-1}, orange-red prism, crystal size 0.28 x 0.16 x 0.14 mm^3, monoclinic, space group *I* 2/a, a = 19.8215(8) Å, b = 44.8370(12) Å, c = 19.8740(5) Å, β = 106.727(3)°, V = 16915.4(5) Å^3, T = 150(2) K, Z = 4, $\rho_{calcd.}$ = 1.174 Mg/m^3, μ (Cu-Kα) = 2.450 mm^{-1}, F(000) = 6260, altogether 26007 reflexes up to h(-24/14), k(-56/52), l(-23/22) measured in the range of 7.480° ≤ Θ ≤ 74.464° , completeness Θ_{max} = 99.7 %, 26007 independent reflections, R_{int} = 0.0349, 10025 reflections with Fo > 4 σ(Fo), 977 parameters, 0 restraints, $R1_{obs}$ = 0.0658, $wR2_{obs}$ = 0.1932, $R1_{all}$ = 0.0926, $wR2_{all}$ = 0.2178, GOOF = 1.062, largest difference peak and hole: 0.978/-0.669 e·Å^{-3}. CCDC 1037697 contains the supplementary crystallographic data for this paper.

General remarks: The collected data only exhibit 86.3% completeness and therefore provide only qualitative structural information. The solid-state structure shows that the complex occupies two orientations in the crystal with respect to the position of the *tert*-butylphenyl substituents. The position of one PF_6 anion (P1A, F1A – F6A, occupancy 38.4 %) partially occupies the same space as the *tert*-butylphenyl substituents (C11B, C60B – C68B) on one side of the molecule. In particular F5A, and C61B and C62B overlap. With the opposite orientation of the complex, instead of occupying the opposite space in the cell, the anion is only slightly shifted to a position close by (P1B, F1B – F6B, occupancy 61.6 %). Additional to the complex cation and PF_6 anions, two molecules of tBuOMe were assigned according to the geometric arrangement of electron density maxima. Positional parameters for the latter had to be restrained in order to achieve a stable refinement. A further

Dalton Transactions Accepted Manuscript

This journal is © The Royal Society of Chemistry 2012

cluster of Q-Peaks was found on a C2 axis and turned out to fill a void that corresponds to the volume of one molecule of tBuOMe.
For the remaining cell space, only few electron density maxima were found which could not be assigned to a meaningful molecular geometry. Also, their intensity was considerably low (Q1 connected to one already assigned solvent molecule, Uij(Q2) = 1.04, Uij(Q3) = 0.76), and the remaining void channels run in between the two disordered positions of the tert-Butyl-phenyl substituents. As mentioned above, the location of solvent molecules in this area depends on and would overlap with the substitutents. Considering the disorder of the latter, we were not able to clearly define all solvent molecules in this area.
Further application of the Platon Squeeze procedure calculated four cavities (one per formula unit) with 27 electrons each for the remaining voids, which suggests the inclusion of half a molecule of tBuOMe per cavity. Further discussion of the unoccupied volume of the disordered t-Bu-phenyl group is neglected in the calculation and partial occupation of additional space could not further be elucidated. In summary, 22 molecules of tBuOMe were added to the unit cell in order to calculate appropriate crystal parameters. It has to be pointed out though that a complete description of this structure cannot be assured and therefore, it is published for principal structural proof only.
TLC: (Silica, acetone/water = 10/1 whereas the later contained 1%$_{vol}$ saturated KNO_3) R_f = 0.15

[(tbbpy)$_2$Ru((tbp)$_2$phen)](PF$_6$)$_2$

For this synthesis a slightly modified literature procedure was used[24]. [(tbbpy)$_2$RuCl$_2$] (50 mg, 0.112 mmol) and phen(tbp)$_2$ (78 mg, 0.110 mmol) were dissolved in a ethanol/water mixture (4/1, 15 mL). The solution was heated to reflux in the microwave (90 W) for 3 hours. Afterwards 68 mg NH_4PF_6 were added and the solvent was narrowed until a red precipitate appeared and the solvent was clear. The precipitate was filtered and recrystallized from acetonitrile and water. **Yield** = 73 % (111 mg); **M** ($C_{44}H_{36}N_6$) = 1372.40 g mol^{-1}; **Anal. Calcd** for $C_{68}H_{80}F_{12}N_6P_2Ru$: C = 59.51, H = 5.88, N = 6.12; found: C = 59.01, H = 6.21, N = 5.99; **MS** (ESI-HRMS): m/z calc. for $C_{68}H_{80}F_{12}N_6P_2Ru$ – 2 (PF_6): 541.27468; found = $[M\text{-}2(PF_6)]^{4+}$ 541.27318 (2.77 ppm); m/z calc. for $C_{68}H_{80}F_{12}N_6P_2Ru$ – (PF_6): 1227.51298; found = $[M\text{-}PF_6]^{4+}$ 1227.51010 (2.35 ppm); **^{1}H-NMR** (400 MHz, ACN-d$_3$, 300 K,): δ = 8.88 (d, *J* = 1.8 Hz, 2H, c), 8.65 (d, *J* = 1.8 Hz, 2H, 3'), 8.57 (d, *J* = 1.7 Hz, 2H, 3), 8.29 (s, 2H, f), 7.96 (d, *J* = 1.8 Hz, 2H, a), 7.85 (d, *J* = 6.0 Hz, 2H, 6'), 7.64 (d, *J* = 6.0 Hz, 2H, 6), 7.52 (m, *J* = 15.1, 5.3 Hz, 10H, d and e and 5'), 7.23 (dd, *J* = 6.0, 1.9 Hz, 2H, 5), 1.47 (s, 18H, *tert.*-butyl.), 1.35 (s, 18H, *tert.*-butyl.), 1.33 (s, 18H, *tert.*-butyl.) ppm. **^{13}C-NMR** (100 MHz, ACN-d$_3$, 300 K): δ = 30.39, 30.49, 31.28, 35.31, 36.19, 36.41, 122.67, 122.87, 125.28, 125.33, 127.42, 128.02, 129.46, 131.65, 133.53, 134.20, 139.12, 147.21, 150.90, 152.43, 152.51, 153.83, 157.66, 158.48, 163.34, 163.67 ppm. **Crystals** suitable for X-ray analysis were obtained from acetonitrile/water. Crystal data for [(tbbpy)$_2$Ru((tbp)$_2$phen)](PF$_6$)$_2$: C_{75} $H_{90.50}$ F_{12} $N_{9.50}$ P_2 Ru, M_r = 1516.07 g mol^{-1}, red fragment, crystal size 0.23 x 0.12 x 0.06 mm^3, triclinic, space group *P* -1, a = 15.7991(4) Å, b = 16.8342(4) Å, c = 16.8521(5) Å, α = 104.461(2)°, β = 116.670(3)°, γ = 92.680(2), V = 3812.4(2) Å^3, T = 180(2) K, Z = 2, $\rho_{calcd.}$ = 1.321 Mg/m^3, μ (Cu-Kα) = 2.711 mm^{-1}, F(000) = 1578, altogether 42405 reflexes up to h(-19/15), k(-20/20), l(-19/21) measured in the range of 7.407° ≤ Θ ≤ 74.493° , completeness Θ_{max} = 99.7 %, 15533 independent reflections, R_{int} = 0.0357, 13862 reflections with Fo > 4 σ(Fo), 979 parameters, 0 restraints, $R1_{obs}$ = 0.0430, $wR2_{obs}$ = 0.1126, $R1_{all}$ = 0.0499, $wR2_{all}$ = 0.1200, GOOF = 1.039, largest difference peak and hole: 1.138/-0.824 e·Å^{-3}. CCDC 1043862 contains the supplementary crystallographic data for this paper. One molecule of acetonitrile was found disordered in the center of the unit cell, which disagrees with the overall inversion symmetry of the rest of the cell. Its geometry was restrained on one largely disordered central carbon atom with fixed coordinates (x = y = z = 0.5) and alternative occupation of the terminal position with either a CH_3 group or nitrogen.

References

1 D. G. Nocera, N. S., *PNAS* **2006**, *103*, 15729–15735.
2 N. Armaroli, V. Balzani, *Angew. Chem. Int. Ed. Engl* **2007**, *46*, 52–66.
3 V. Balzani, A. Credi, M. Venturi, *ChemSusChem* **2008**, *1*, 26–58.
4 T. R. Cook, D. K. Dogutan, S. Y. Reece, Y. Surendranath, T. S. Teets, D. G. Nocera. *Chem. Rev. 2010*, **110**, 6474–6502.
5 K. Yamauchi, S. Masaoka, K. Sakai, *J. Am. Chem. Soc.* **2009**, *131,* 8404–8406.
6 S. Rau, B. Schäfer, D. Gleich, E. Anders, M. Rudolph, M. Friedrich, H. Görls, W. Henry, J. G. Vos *Angew. Chem. Int. Ed. Engl,* **2006**, *45*, 6215–6218.
7 P. Belser, R. Dux, M. Baak, L. De Cola, V. Balzani, *Angew. Chem. Int. Ed. Engl.* **1995**, *34*, 595–598.
8 H. Ozawa, M. Haga, K. Sakai, *J. Am. Chem. Soc.* **2006**, *128*, 4926–4927.
9 C. V. Suneesh, B. Balan, H. Ozawa, Y. Nakamura, T. Katayama, M. Muramatsu, Y. Nagasawa, H. Miyasaka, K. Sakai, *Phys. Chem. Chem. Phys.* **2013**, *16*, 1607–1616.
10 H. Ozawa, K. Sakai, *Chem. Commun.* **2011**, *47*, 2227–2242.
11 S. Rau, D. Walther, J. G. Vos, *Dalton Trans.* **2007**, 915–919.
12 S. Tschierlei, M. Presselt, C. Kuhnt, A. Yartsev, T. Pascher, V. Sundström, M. Karnahl, M. Schwalbe, B. Schäfer, S. Rau, M. Schmitt, B. Dietzek, J. Popp, *Chem. Eur. J.* **2009**, *15*, 7678–7688.
13 S. Tschierlei, M. Karnahl, M. Presselt, B. Dietzek, J. Guthmuller, L. González, M. Schmitt, S. Rau, J. Popp, *Angew. Chem. Int. Ed. Engl.* **2010**, *49*, 3981–3984.
14 M. Karnahl, C. Kuhnt, F. W. Heinemann, M. Schmitt, S. Rau., J. Popp, B. Dietzek, *Chem. Phys.***2012**, *393*, 65–73.
15 C. Chiorboli, C. A. Bignozzi, F. Scandola, *Inorg. Chem.* **1999**, *38*, 2402–2410
16 M. Karnahl, C. Kuhnt, F. Ma, A. Yartsev, M. Schmitt, B. Dietzek, S. Rau, J. Popp, *Chemphyschem* **2011**, *12*, 2101–2109.
17 J. M. Lehn in *Supramolecular chemistry: Concepts and Perspectives*. Wiley-VHC, Weinheim, **1995**.
18 V. Balzani in *Electron transfer in chemistry:* Wiley-VCH, Weinheim, **2001**, vol. 5.
19 J. R. Fisher, D. J. Cole-Hamilton, *J. Chem. Soc. Dalt. Trans.* **1984**, 809-813.
20 E. Amouyal, A. Homsi, J. Chambron, J. Sauvage, *J. Chem. Soc. Dalt. Trans.* 1990, 1841-1845.
21 Y. Sun, D. Lutterman, C. Turro, *Inorg. Chem.* **2008**, *47*, 6427–6434.
22 C. Chiorboli, M. Rodgers, F. Scandola, *J. Am. Chem. Soc.* 2003, *125*, 483–491.
23 J. Bolger, A. Gourdon, E. Ishow, J. Launay, *Inorg. Chem.* **1996**, *35*, 2937–2944.
24 M. Karnahl, S. Tschierlei, C. Kuhnt, B. Dietzek, M. Schmitt, J. Popp, M. Schwalbe, S. Krieck, H. Görls, F. W. Heinemann S. Rau, *Dalton Trans.* **2010**, *39*, 2359–2370.
25 J. Frey, T. Kraus, V. Heitz, J.-P. Sauvage, *Chem. Eur. J.* **2007**, *13*, 7584–7594.
26 M. G. Pfeffer, L. Zedler, S. Kupfer, M. Paul, M. Schwalbe, K. Peuntinger, D. M. Guldi, J. Guthmuller, J. Popp, S. Graefe, B. Dietzek, S. Rau, Dalton Trans. **2014**, *43*, 11676-11686.
27 N. Komatsuzaki, R. Katoh, Y. Himeda, H. Sugihara, H. Arakawa, K. Kasuga, *J. Chem. Soc. Dalt. Trans.* 2000, 3053–3054.
28 D. Gut, A. Rudi, J. Kopilov, I. Goldberg, M. Kol*, J. Am. Chem. Soc* **2002**, *124*, 5449-5456.
29 S. D. Bergman, D. Reshef, L. Frish, Y. Cohen, I. Goldberg, M. Kol, *Inorg. Chem.* **2004**, *43*, 3792-3794.
30 S. D. Bergman, M. Kol, *Inorg. Chem.* **2005**, *44*, 1647-1654

Dalton Transactions Accepted Manuscript

[31] S. D. Bergman, D. Gut, M. Kol, C. Sabatini, A. Barbieri, F. Barigelletti, *Inorg. Chem.* **2005**, *44*, 7943-7950.

[32] C. A. Hunter, J. K. M. Sanders, *J. Am. Chem. Soc.* **1990**, *112,* 5525-5534.

[33] P. Douglas, J. F. Stoddart, *Angew. Chem. Int. Ed. Engl.* **1996**, *35*, 1154-1196.

[34] S. Burley, G. Petsko, *Science*, **1985**, 23-28.

[35] G. R. Desiraju in *Crystal Engineering: Design of Organic Solids*; Elsevier, Amsterdam, **1989**.

[36] H. Krass, E. A. Plummer, J. M. Haider, P. R. Baker, N. V. Alcock, Z. Pikramenou, M. J. Hannon, D. G. Kurth, *Angew. Chem. Ind. Ed. Engl.* **2001**, *40*, 3862–3865.

[37] U. H. F. Bunz, J. U. Engelhart, B. D. Lindner, M. Schaffroth, *Angew. Chem. Int. Ed*. **2013**, *52*, 3810 – 3821.

[38] W. Pisula, X. Feng, K. Müllen, *Chem. Mater.*, **2011**, *23*, 554–567.

[39] H. Liu, P. J. Sadler, *Accounts of chemical Research* **2011**, *44*, 349-359.

[40] U. H. F. Bunz, *Pure Appl. Chem.* **2010**, *82*, 953–968.

[41] J.-L. Brédas, D. Beljonne, V. Coropceanu, J. Cornil, *Chem. Rev.* 2004, *104*, 4971–5004.

[42] S. M. Draper, D. J. Gregg, E. R. Schofield, W. R. Browne, M. Duati, J. G. Vos, P. Passaniti, *J. Am. Chem. Soc.* **2004**, *126*, 8694-8701.

[43] A. Chouai, S. E. Wicke, C. Turro, J. Bacsa, K. R. Dunbar, D. Wang, R. P. Thummel, *Inorg. Chem.* **2005**, *44*, 5996-6003.

[44] M. J. Hannon, C. L. Painting, E. A. Plummer, L. J. Childs, N. W. Alcock, *Chem. Eur. J.* **2002**, *8*, 2225-2238.

[45] M. Pascu, G. J. Clarkson, B. M. Kariuki, M. J. Hannon, *Dalton Trans.* **2006**, 2635-2642.

[46] D. G. Kurth, *Sci. Technol. Adv. Mater.* **2008**, *9*, 014103.

[47] L. Duan, F. Bozoglian, S. Mandal, B. Stewart, T. Privalov, A. Llobet, L. Sun, *Nature chem.* **2012**, *4*, 418-423.

[48] C. J. Richmond, R. Matheu, A. Poater, L. Falivene, J. Benet-Buchholz, X. Sala, L. Cavallo, A. Llobet, *Chem. Eur. J.* **2014**, *20*, 17282 – 17286.

[49] B. Schäfer, H. Görls, S. Meyer, W. Henry, J. G. Vos, S. Rau, *Eur. J. Inorg. Chem.* **2007,** 4056–4063.

[50] S. Ott, R. Faust, *Synthesis* **2005**, 3135–3139.

[51] F. R. Keene, *Chem. Soc. Rev.* **1998**, *27*, 185-193.

[52] J. Bolger, A. Gourdon, E. Ishow, J. Launay, *J. Chem. Soc. Chem. Commun.* **1995**, *20*, 1799-1800.

[53] M. O. Sinnokrot, C. D. Sherrill, *J. Phys. Chem. A*, 2004, **108**, 10200-10207.

[54] V. Steullet and D. W. Dixon, *Chem. Soc., Perkin Trans. 2,* 1999, 1547.

[55] J.-S. Chen and R. B. Shrits, *The Journal of Physical Chemistry*, 1985, **89**, 1643.

[56] M. Pfeffer, C. Pehlken, R. Staehle, D. Sorsche, C. Streb, S. Rau, *Dalton. Trans.*, 2014, **43**, 13307-13315.

[57] This constant is different (289 ± 17 M^{-1} against 122 ± 19 M^{-1}) from the one described in the mentioned article, because of a modified and improved methodology and by the use of more data points (see paragraph 3 of the supporting information).

[58] S, Bodige, A. S. Torres, D. J. Maloney, D. Tate, G. R. Kinsel, A. K. Walker, F. M. MacDonnell, *J. Am. Chem. Soc.* **1997**, *119*, 10364–10369).

[59] M. Karnahl, S. Krieck, H. Görls, S. Tschierlei, M. Schmitt, J. Popp, D. Chartrand, G. S. Hanan, R. Groarke, J. G. Vos, S. Rau, *Eur. J. Inorg. Chem.* **2009,** 4962–4971.

[60] S. Campagna, F. Puntoriero, F. Nastasi, G. Bergamini, V. Balzani in Topics in Current Chemistry: *Photochemistry and Photophysics of Coordination Compounds I* **2007**, *280*, 117–214.

[61] A. Juris, V. Balzani, F. Barigelletti, S. Campagna, P. Belser, A. von Zelewsky, *Coord. Chem. Rev.* **1988**, *84*, 85-277.

[62] C. Kuhnt, M. Karnahl, S. Rau, M. Schmitt, B. Dietzek, J. Popp, *Chem. Phys. Lett.* **2011**, *516*, 45–50.

[63] C. Kuhnt, M. Karnahl, M. Schmitt, S. Rau, B. Dietzek, J. Popp, *Chem. Commun.* **2011**, *47*, 3820-3821.

[64] S. Rau, B. Schäfer, A. Grüßing, S. Schebesta, K. Lamm, J. Vieth, H. Görls, D. Walther, M. Rudolph, U. W. Grummt, E. Birkner, *Inorg. Chim. Acta* **2004**, *357*, 4496–4503.

[65] N. R. de Tacconi, R. Chitakunye, F. M. MacDonnell, R. O. Lezna, J. *Phys. Chem. A* **2008**, *112*, 497-507.

[66] T. Ishi-i, T. Hirayama, K. Murakami, H. Tashiro, T. Thiemann, K. Kubo, A. Mori, S. Yamasaki, T. Akao, A. Tsuboyama, T. Mukaide, K. Ueno, S. Mataka, *Langmuir* , **2005**, *21*, 1261–1268.

[67] B. P. Sullivan, D. J. Salmon, T. J. Meyer, *Inorg. Chem.* **1978**, *17*, 3334–3341.

[68] P. J. Giordano, C. R. Bock, M. S. Wrighton, *J. Am. Chem. Soc.* **1978**, *100*, 6960–6965.

[69] S. Bodige, F. M. MacDonnell, *Tetrahedron Lett.* **1997**, *38*, 8159–8160.

[70] P. Comba, R. Krämer, A. Mokhir, K. Naing, E. Schatz, *Eur. J. Inorg. Chem.* **2006,** 4442–4448.

[71] G. M. Sheldrick, *Acta Cryst*. **2008**, *A64*, 112-122.

[72] a) A. L. Spek, *J. Appl. Cryst.* **2003**, *36*, 7-13; b) A. L. Spek. *Acta Cryst.* **2009**, *D65*, 148-155.

Dalton Transactions Accepted Manuscript

This journal is © The Royal Society of Chemistry 2012